

Lattice Knots in a Slab

D. Gasumova[†], E. J. Janse van Rensburg^{†§} and A. Rechnitzer[‡]

[†]Department of Mathematics and Statistics, York University
Toronto, Ontario M3J 1P3, Canada

rensburg@yorku.ca

[‡]Department of Mathematics, The University of British Columbia
Vancouver V6T 1Z2, British Columbia , Canada
andrew@math.ubc.ca

Abstract. In this paper the number and lengths of minimal length lattice knots confined to slabs of width L , is determined. Our data on minimal length verify the results by Ishihara et. al. [8] for the similar problem, except in a single case, where an improvement is found. From our data we construct two models of grafted knotted ring polymers squeezed between hard walls, or by an external force. In each model, we determine the entropic forces arising when the lattice polygon is squeezed by externally applied forces. The profile of forces and compressibility of several knot types are presented and compared, and in addition, the total work done on the lattice knots when it is squeezed to a minimal state is determined.

§ To whom correspondence should be addressed (rensburg@yorku.ca)

1. Introduction

Chemically identical ring polymers may be knotted and these are examples of topological isomers which may have chemical and physical properties determined by their topology. There has been a sustained interest in the effects of knotting and entanglement in polymer physics and chemistry, and it is known that entanglements may play an important role in the chemistry and biological function of DNA [29]. For example, entanglement and knotting are active aspects of the functioning of DNA and are mediated by topoisomerases [16, 17], while proteins are apparently rarely knotted in their natural active state [26].

Ring polymers with specified knot type have been chemically synthesized [5], but more often, random knotting of ring polymers occurs in ring closure reactions [23, 2, 20]. In this case, a spectrum of knot types are encountered [28, 6, 24], and these are a function of the length of the polymer: Numerical studies show that longer ring polymers are knotted with higher frequency and complexity [14].

Ring polymers adsorbing in a plane or compressed in a slab also appear to have increasing knot probability [19, 21], although the probability may decrease in very narrow slabs [27]. Similar effects are seen when a force squeezes a ring polymer in a slab [10], and the results of the calculation in reference [9] suggest that knotted polygons will exert higher entropic forces on the walls of a confining slit. More generally, the phase behaviour of lattice ring polymers confined to slabs and subjected to external forces were examined in reference [25].

The entropic force of a knotted ring polymer confined to a slab between two plates were examined using a bead-spring model in reference [18]. In this study it was found that more complex knot-types in a ring polymer exert higher forces on the confining walls of the slab (if the slab is narrow).

In this paper we obtain qualitative results on the entropic properties of tightly knotted polymers confined to a slab or squeezed by a flexible membrane, using minimal length cubic lattice knots. We will consider two different models.

The first is a model of a tightly knotted ring polymer of fixed length squeezed between two hard walls or plates (see figure 1). Steric repulsions between monomers in the polymer are due to self-avoidance and to the (self)-entanglement of the polymer, and will induce a restorative force on the walls. This force will also contain an entropic contribution, since the polymer loses entropy as monomers approach one another when the walls of the slab is squeezed together. An externally applied force will overcome this entropic repulsion at critical magnitudes, and we shall determine these critical forces for several knot types in our model. An external force will tend to squeeze the walls of the slab together, and at some critical widths of the slab, the polymer cannot shrink further without expanding laterally and increasing its length. Beyond this critical width there may also be an elastic energy contribution to the free energy – the polymer stretches in length to accommodate the narrow slab. We model this with a Hooke energy.

The second model is inspired by the study in reference [7]. In figure 1 therein, a polymer is grafted to a hard wall and covered by a soft flexible membrane. The membrane may be modeled by a hard wall as in the first model above. On the other hand, a pressure difference across the membrane will induce forces on the monomers in the top layer of the grafted polymer. This couples the force to the height of the monomers in the top layer – the force is mediated directed through the membrane and push on the highest monomers of the polymer.

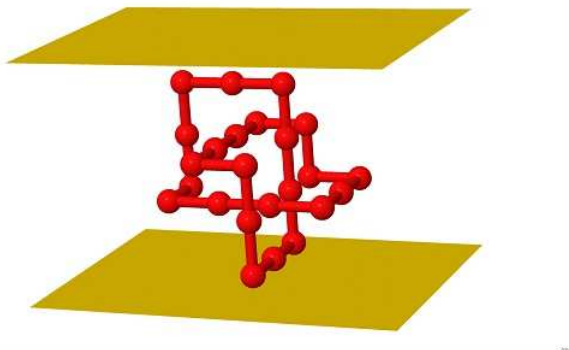


Figure 1. A minimal length lattice knot of type 3_1 squeezed between two hard walls. The lattice knot is grafted to the bottom wall – that is, it has at least one vertex in this wall. If the two hard walls are a distance L apart, then the height of the lattice knot is $h \leq L$, since the polygon must fit between the two walls. The number of these lattice knots of length n are denoted $p_n^L(K)$.

We consider the models presented above and illustrated in figures 1 and 2 in turn. In section 2 we present our models and discuss the collection of numerical data. An implementation of the GAS-algorithm for knotted cubic lattice polygons in slabs [11] was used, and we collected data on the entropy and minimal length of knotted lattice polygons up to eight crossings. Our data verify similar results obtained in reference [8]. In section 3 we discuss the first model and present our data, and in section 4 we present data on the second model and discuss our results. The paper is concluded in

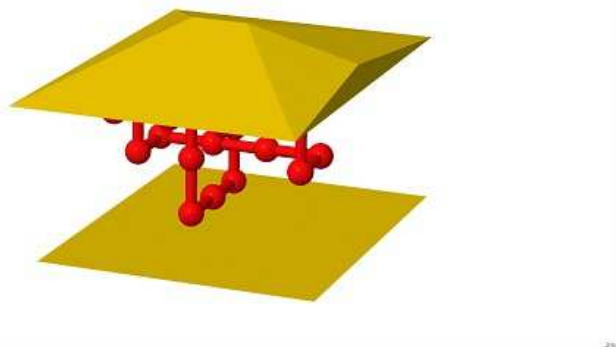


Figure 2. A minimal length lattice knot of type 3_1 grafted to the bottom wall and covered by a weightless flexible membrane. The lattice knot is grafted to the bottom wall (which is hard) by having at least one vertex in this wall. A pressure gradient over the top membrane will exert a force compressing the knot onto the bottom wall. The force is mediated through the membrane onto the monomers in the top layer of the lattice knot. If the height of the lattice knot is h , then the number of vertices at height h is conjugate to a force pushing the lattice knot towards the bottom wall. The number of these lattice knots of length n is denoted by $p_n(K; h)$.

section 5.

2. Models of lattice knots in slabs

A lattice polygon is a sequence $\omega_n = \{v_0, v_1, \dots, v_{n-1}\}$ of distinct vertices v_i such that $v_i v_{i+1}$, for $i = 0, 1, \dots, n-2$ and $v_{n-1} v_0$ are unit length edges in the cubic lattice \mathbb{Z}^3 . Two polygons ω_0 and ω_1 are equivalent if they are translates of each other. The length of a polygon is its number of edges (or steps). A polygon is, by inclusion, a tame embedding of the unit circle in \mathbb{R}^3 and so has a well defined knot type. A lattice polygon with specified knot type is a *lattice knot*.

The number of distinct polygons of length n and knot type K will be denoted $p_n(K)$. For example $p_4(0_1) = 3$ while $p_n(0_1) = 0$ if $n < 4$ or if n is odd, where 0_1 is the unknot in standard knot notation. It is also known that $p_{24}(3_1^+) = 1664$ while $p_n(3_1^+) = 0$ if $n < 24$ [22], where 3_1^+ is the trefoil knot type. By symmetry, $p_n(K^+) = p_n(K^-)$ if K is a chiral knot type.

The *minimum length* of a lattice knot K is the minimum number of edges required to realise it as a polygon in \mathbb{Z}^3 . For example, the minimal length of knot type 0_1 is 4 and of knot type 3_1^+ or 3_1^- is 24 edges. The minimal length is denoted by n_K , so that $n_{0_1} = 4$ and $n_{3_1^+} = 24$ [4]. It is also known that $n_{4_1} = 30$ (4_1 is the figure eight knot) and $n_{5_1^+} = 34$ [22]. Beyond these, only upper bounds on n_K are known.

If $v \in \omega_n$ is a vertex in a lattice polygon, then the Cartesian coordinates of v are $(X(v), Y(v), Z(v))$. A polygon is *grafted* to the XY plane $Z = 0$ if $Z(v) \geq 0$ for all vertices v in ω , and there exists one vertex, say v_0 , such that $Z(v_0) = 0$. The *height* of a grafted polygon is $h = \max \{Z(v) \mid v \in \omega_n\}$.

A grafted polygon ω_n is said to be confined to a slab \mathbb{S}_L of width L if $0 \leq Z(v) \leq L$ for each vertex $v \in \omega_n$. A polygon confined to a slab is illustrated in figure 1, where the *bottom wall* and *top wall* of the slab are indicated.

Next we define the number of polygons of length n , knot type K , and confined in a slab of width L by $p_n^L(K)$. Similarly, define the number of polygons of length n , knot type K , and of height h by $p_n(K; h)$. Clearly,

$$p_n^L(K) = \sum_{h \leq L} p_n(K; h). \quad (1)$$

The minimal length of a lattice knot in a slab of width L will be denoted $n_{L,K}$. For example, one may deduce that $n_{2,3_1} = 24$ from reference [4]. However, simulations show that $n_{1,3_1} = 26$ [8]. In other words, in a slab of width $L = 1$, it is necessary to have a polygon of length 26 to tie a lattice trefoil, while if $L \geq 2$ then 24 edges will be sufficient (and necessary) [4].

With these definitions, we define two models of grafted lattice knots. The first model is that of a grafted lattice knot in a slab with hard walls (see figure 1). In this model the confinement of the lattice knot will decrease its entropy, and this will induce an entropic repulsion between the top and bottom walls of the slab. The discrete geometry in this model implies that the induced entropic force is given by free energy differences if the distance between the walls is decreased by one step.

The second model is illustrated in figure 2. The grafted lattice knot is covered by a flexible and weightless membrane. A (positive) pressure difference in the fluid above and below the membrane induces a force pushing on the top vertices in the lattice knot. A negative pressure difference in the fluid results in an effective pulling force on the vertices in the top layer of the lattice knot. In this model, the partition function is

given by all the states of grafted lattice knot (including those of any height). The force f induced by the pressure difference will push on the highest vertices in the polygon as it is mediated by the flexible lightweight membrane onto these vertices. A (linear) compressibility of the lattice knot can be determined by taking second derivatives of the free energy of this model to the applied force, as we shall show below.

2.1. Numerical approach

In this paper we examine the properties of minimal length lattice knots squeezed between two hard walls, or squeezed by an applied force towards a hard wall. In both these models it is necessary to determine the number and length of lattice knots in slabs of width L . Some data of this kind were obtained in reference [8], and we will at the same time verify in most cases, and improve in one case, on their results.

Our numerical approach will be the implementation of the GAS-algorithm for lattice knots [11, 12, 13] using BFACF elementary moves [1, 3]. The lattice knots will be confined to slab \mathbb{S}_L of width L defined by $\mathbb{S}_L = \mathbb{Z}^2 \times \{0, 1, \dots, L\}$. We implement the algorithm by noting that BFACF elementary moves on unrooted cubic lattice polygons are known to have irreducibility classes which are the knot types of the polygons. The proof of this fact can be found in reference [15]. Note that the proof in reference [15] applies *mutatis mutandis* to the model in this paper as well, provided that $L \geq 2$.

We estimate $p_{n_{L,K}}(K; h)$ (the number of polygons of knot type K , height h and of length $n_{L,K}$) using the GAS algorithm for knotted polygons. Here $n_{L,K}$ is the minimal length of grafted lattice knots of type K in a slab of width L . By summing $h \leq L$, one obtains $p_{n_{L,K}}^L(K)$, the number of grafted lattice knots of type K which can fit in a slab of width L , of length $n_{L,K}$ (and thus of height $h \leq L$). Our results are not rigorous, and in a strict sense the results of $n_{L,K}$ are upper bounds while $p_{n_{L,K}}(K; h)$ are lower bounds. Since the GAS algorithm can be implemented as a flat histogram method, it is efficient at rare event sampling and thus at finding knotted polygons of minimal length. A comparison of our results with the data in reference [8] makes us confident that our results are exact in almost all cases.

Data on lattice knots in slabs \mathbb{S}_L , with $L \geq 2$ can be collected as in reference [12]. The case $L = 1$ requires further scrutiny. Data in this ensemble were collected by generating lattice knots in \mathbb{S}_2 , and sieving out lattice polygons which fit into \mathbb{S}_1 . By biasing the sampling to favour polygons which fit into \mathbb{S}_1 , we were successful in generating lists of lattice knots in \mathbb{S}_1 . We are reasonably confident that in most cases our lists of knotted polygons are complete.

We display our data on the minimal length of lattice knots in \mathbb{S}_L in appendix A in tables 5 and 7 (for some compound knots). The data in table 5 agree for all knot types, except for 8_{18} , with the data in reference [8]. We improved on the estimate for the minimal length of 8_{18} in \mathbb{S}_1 by finding states at length $n = 70$, compared to 72 in that reference.

As one might expect, we observe a steady increase of $n_{L,K}$ with decreasing L for each knot type, and also down table 5. Decreasing L squeezes lattice knots in narrower slabs, and at critical values of L there is an increase in the minimal length. For example, for the trefoil knot 3_1^+ , there are realizations of lattice knots with this knot type at $n = 24$ edges for $L \geq 2$. However, if $L = 1$, then 26 edges are needed. In figure 3 the minimal lengths of lattice knots in \mathbb{S}_1 are compared to the minimal lengths of lattice knots in the bulk lattice. In this scatter plot each knot type has coordinates

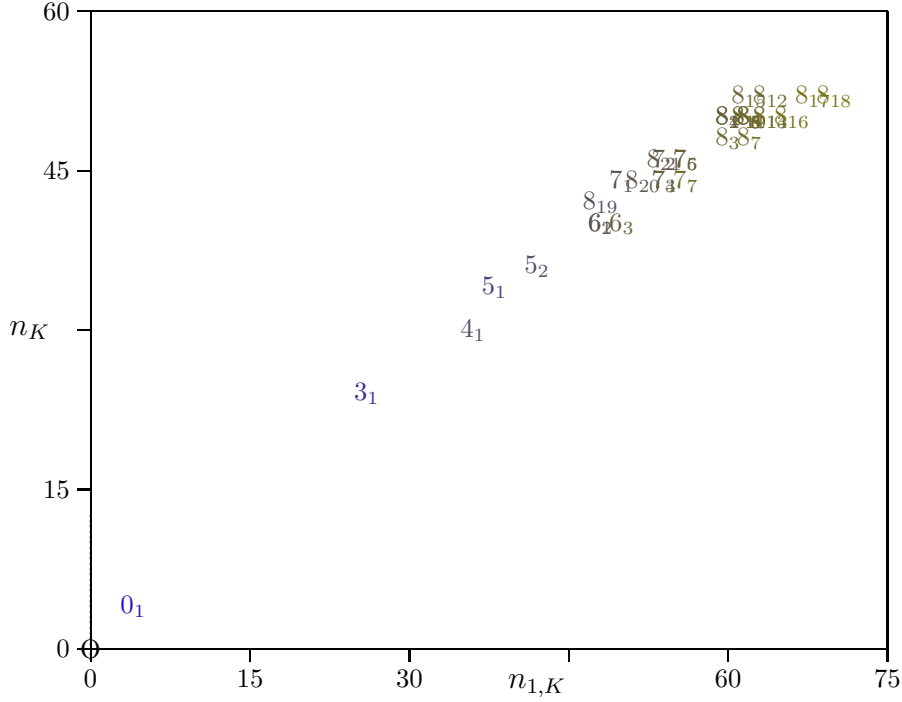


Figure 3. A scatter plot of minimal lengths $n_{1,K}$ in \mathbb{S}_1 (X -axis) and minimal lengths n_K (Y -axis).

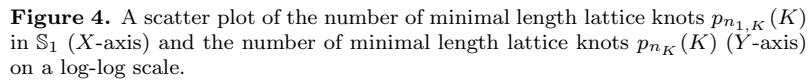
$(n_{1,K}, n_K)$. We found that $n_{1,K} > n_K$ for all non-trivial knot types, but the data do cluster along a line showing a strong correlation between these two quantities. For slabs \mathbb{S}_L our data are displayed in table 5, showing that $n_{1,K} \geq n_{L,K} \geq n_K$ generally.

Naturally, $n_{L,K}$ is a non-increasing function of L for a given knot type K . In some cases there is a large increase in $n_{L,K}$ with decreasing L . For example, 8_{18} increases from 52 at $L = 4$ through 56, 60 and to 70 as L decreases through 3, 2 and 1.

The number of lattice knots of minimal length in \mathbb{S}_L are displayed in tables 6 and 8 (for some compound knots) in the appendix. We display some of these results in figure 4, where we plot the number of minimal length lattice knots against the number of minimal length lattice knots in \mathbb{S}_1 for different knot types on a log-log scale. The data scatter in the plot, showing that the number of minimal length lattice knots may change significantly with a decrease in L .

Lattice knots are partitioned into symmetry classes due to invariance under rotations or (in the case of amphichiral knots) reflections which respect the orientation of \mathbb{S}_L . Thus, the sets of lattice knots enumerated in tables 6 and 8 partition into symmetry classes. These classes are listed in tables 9 and 10 in the appendix. The symmetry classes are denoted by $2^a 4^b 6^c 8^d 12^e 16^f$ for each set of lattice knots. For example, for the knot type $3_1^+ \# 3_1^+$ in table 9 and for $L = 1$, the symmetry classes are $2^3 4^3 6^8 8^{285}$ meaning that there are 3 classes with two members (each member is a lattice knot), 36 classes with 4 members and 285 with 8 members.

The data show that the entropy decreases with decreasing L , if the minimum length of the polygon does not change. In cases where the minimum length increases with decreasing L , it may be accompanied by a large decrease or increase in entropy.



In what follows, we will use the data in these tables to determine the response of the lattice knots when forces are applied to squeeze them in slabs with hard walls, or in a model where the forces are mediated via a flexible membrane to the highest vertices in the lattice knots.

The free energy of grafted lattice knots in a slab of width L is given by

The lattice knots have fixed length (this is the canonical ensemble), and we assume in this model that the length is fixed at the minimal length in the slab \mathbb{S}_L .

We assign an energy to the lattice knot as follows: Compressing a minimal length lattice knot in a slab of width L will generally reduce its entropy, but at a minimum value of L , no further compression can take place because a minimal length lattice knot cannot be realised in a narrower slab. Instead, further increase of pressure on the \mathbb{S}_L will induce forces along the edges of the polygon, and at a critical value of the force, these induced forces will overcome the elastic or tensile strength of the edges composing the lattice knot. The result is that the lattice knot will either stretch in length to fit in a narrower slab, or it will break apart and be destroyed. We assume the former case (our data show that in most cases the level of stretching is less than 10% of the rest length of the lattice polygon). Thus, assign a Hooke energy to the

polygon, with rest length equal to n_K . The energy is then given by

$$\text{Energy} = k \cdot (n_{L,K} - n_K)^2, \quad (3)$$

where $n_{L,K}$ is the minimum length to accommodate the lattice knot in a slab of width L . There is no Hooke energy in the event that $n_{L,K} = n_K$.

With the above in mind, we define the free energy as follows

$$\mathcal{F}_L = k(n_{L,K} - n_K)^2 - T \log p_{n_{L,K}}^L(K). \quad (4)$$

For example, in the case of the unknot 0_1 , one may determine directly that $n_{0_1} = 4$ and $p_{n_{0_1}} = 1$ while $p_{n_{1,0_1}} = 3$. This shows that $\mathcal{F}_0 = -T \log 1 = 0$ and $\mathcal{F}_1 = -T \log 3$.

It is important to note that this free energy is a low temperature or a stiff Hooke spring approximation. It is low temperature because thermal fluctuations in the length of the lattice knot are not modeled (that is, the lattice knot is always in the shortest possible conformations in \mathbb{S}_L), and it is a stiff Hooke spring approximation for that same reason: the energy barrier to stretch the polygon to $n_{L,K} + 2$ edges in length is too big, and those states do not make a measurable contribution to the free energy.

Free energy differences as a result change in entropy and the Hooke term induces entropic forces pushing against the walls of the slab. These forces should push the walls apart, both decreasing the length of the lattice knot and increasing its entropy. They are given by

$$F_L = \Delta_1 \mathcal{F}_L = \mathcal{F}_L - \mathcal{F}_{L-1}. \quad (5)$$

If an externally applied force f squeezing the walls of \mathbb{S}_L together exceeds F_L (that is, if $|f| > |F_L|$), then the force f will overcome the entropic and Hooke terms in the free energy and squeeze the lattice knot into \mathbb{S}_{L-1} . Thus, the critical values of an applied force pushing against F_L are given when

$$f_L = -F_L \quad (6)$$

and if $|f| > |f_L|$ then the walls of \mathbb{S}_L will be squeezed together to compress the lattice knot. We call f_L the *critical force* of the model.

Compressing the lattice knot between two hard walls performs work on the knot, and conversely, if a lattice knot is placed in a narrow slab and the slab expands as a result, then the lattice knot performs work on the walls of the slab. The maximum amount of useful work that can be extracted from this process is given by

$$\mathcal{W}_K = \sum_L f_L \cdot \delta L \quad (7)$$

assuming that the expansion is isothermic and reversible. In our geometry, $\delta L = 1$. Thus, \mathcal{W}_K reduces to $\sum_L f_L$.

For example, compressing a minimal length unknotted polygon between two hard walls reduces the entropy of the unknot polygon only when L transitions from 1 to 0. That is, the top wall in figure 1 can be pushed down without encountering resistance until $L = 1$. Further compressing to $L = 0$ reduces the free energy by

$$F_1 = \Delta_1 \mathcal{F}_1 = (\mathcal{F}_1 - \mathcal{F}_0) = -T \log 3. \quad (8)$$

This shows that the critical force is $f_1 = T \log 3$ in this model. In this case, the unknot lattice polygon can do at most $\mathcal{W}_{0_1} = T \log 3$ units of work, assuming that it is placed in \mathbb{S}_0 and allowed to expand the slab.

3.1. Squeezing minimal length lattice trefoils between two planes

These ideas can be extended to lattice knots, using the data in tables 5 and 6.

In the case of the trefoil knot 3_1^+ , it follows from table 5 that $n_{L,3_1^+} = 24$ if $L \geq 2$ but that $n_{1,3_1^+} = 26$. In other words, the length of the lattice knot increases from 24 to 26 if it is squeezed by a force into a slab \mathbb{S}_1 . This stretching of the polygon stores work done by the compressing force in the form of elastic energy, which we indicate by the Hooke term in equation (4).

If the compressing force is removed, the lattice knot will rebound to length 24, and expand the slab to width $L = 2$, performing work while doing so. In $L = 2$ the lattice knot is not stretched, but it still suffers a reduction in entropy. Further expansion of the slab width to $L = 3$ increases entropy, and there is thus an entropic force pushing the hard walls apart until the lattice knot enters a state of maximum entropy for values of L large enough.

With this in mind, the free energies of minimal length lattice knots of type 3_1^+ as a function of L may be obtained from the data in tables 5 and 6. The results are

$$\begin{aligned}\mathcal{F}_1(3_1^+) &= 4k - T \log 36; \\ \mathcal{F}_2(3_1^+) &= -T \log 152; \\ \mathcal{F}_3(3_1^+) &= -T \log 1660; \\ \mathcal{F}_{\geq 4}(3_1^+) &= -T \log 1664.\end{aligned}$$

Observe the steady increase in the entropy of the lattice knot with increasing L . At $L = 2$ the knot cannot be compressed to $L = 1$ without increasing its length to 26 edges, and the Hooke term $4k$ appears in $\mathcal{F}_1(3_1^+)$.

From the above data one may compute the critical forces for lattice knots of type 3_1^+ . These are

$$f_L = \begin{cases} \infty, & \text{if } L = 1; \\ 4k + T \log(38/9), & \text{if } L = 2; \\ T \log(415/38), & \text{if } L = 3; \\ T \log(416/415), & \text{if } L = 4; \\ 0, & \text{if } L \geq 5. \end{cases} \quad (9)$$

The results for f_L above show that there is no entropy loss with decreasing L until $L = 4$. Thereafter, compressing the lattice knot results in entropy loss, and the critical forces are given above. At $L = 2$ the knot stretches to accommodate conformations in $L = 1$, with the result that a Hooke term appears. Observe that $f_1 = \infty$, since a non-trivial lattice knot cannot be squeezed into \mathbb{S}_0 , unless the compressing force overcomes the strength of the edges and breaks the polygon apart.

The above expressions for the critical forces gives a compression profile for squeezing the lattice trefoil between two planes. We illustrate this profile as a bargraph in figure 5 – where we put $k = 1/4$ and $T = 1$. In this case one may also compute $\mathcal{W}_{3_1^+} = 4k + T \log(416/9)$. The choice of $k = 1/4$ in figure 5 gives a Hooke contribution of one to the free energy if the polygon should stretch by two edges. At this level, the Hooke energy does not dominate the free energy.

Similar data can be obtained for the figure eight knot 4_1 , and its critical forces

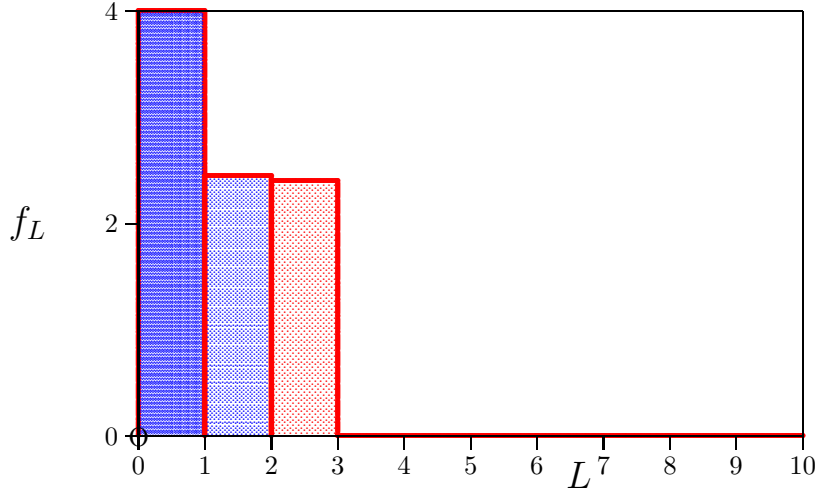


Figure 5. A profile of critical forces f_L for the lattice knot of type 3_1^+ . Compressing the knot between two plates encounters no resistance for $L \geq 5$. If $L = 4$, then there is a small resistance (not visible on this scale), and for $L \leq 3$ a larger resistance. Bars in red indicate that the critical forces are due to entropy reduction alone, and blue bars denote a Hooke contribution to the critical force. In this example, $k = 1/4$ and $T = 1$.

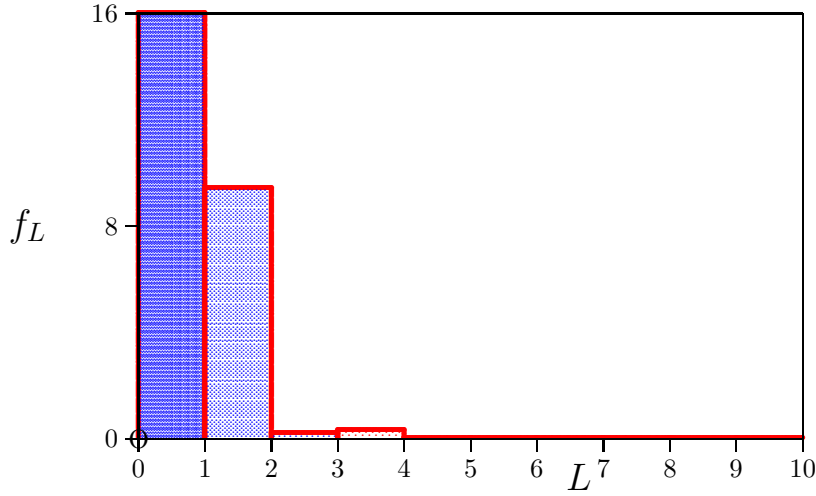


Figure 6. A profile of critical forces f_L for the lattice knot of type 4_1 . Compressing the knot between two plates encounters no resistance for $L \geq 5$. If $L = 4$, then there is a small resistance, and for $L \leq 3$ a larger resistance. Bars in red indicate that the critical forces are due to entropy reduction alone, and blue bars denote a Hooke contribution to the critical force. In this example, $k_1 = k_2 = 1/4$ and $T = 1$.

are give by

$$f_L = \begin{cases} \infty, & \text{if } L = 1; \\ 32k + T \log(758/185), & \text{if } L = 2; \\ 4k - T \log(379/170), & \text{if } L = 3; \\ T \log(114/85), & \text{if } L = 4; \\ 0, & \text{if } L \geq 5, \end{cases} \quad (10)$$

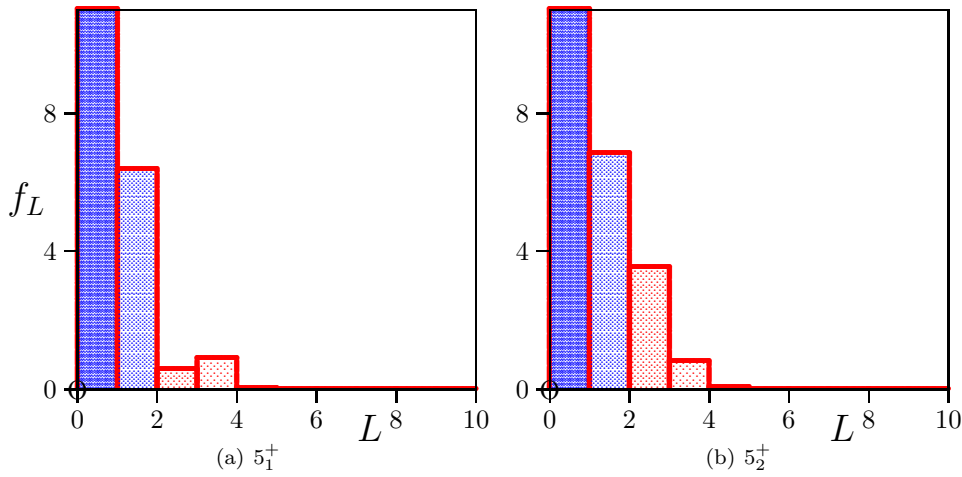


Figure 7. A profile of critical forces f_L for lattice knots of types 5_1^+ and 5_2^+ . There is no resistance to compression until $L = 5$. There are small resistances if $L = 4$, and this decreases even further for $L = 3$ in the case of 5_1^+ . In the case of 5_2^+ the resistance increases with decreasing L . Bars in red indicate that the critical forces are due to entropy reduction alone, and blue bars denote a Hooke contribution to the critical force. In this example, $k = 1/4$ and $T = 1$.

displayed in figure 6.

In this knot type, the lattice knot increases in length both in the transition from $L = 3$ to $L = 2$, and then again to $L = 1$, as seen in table 5. While one will generally expect $f_L \geq f_{L+1}$ (that is, a larger force is necessary to compress the knot in narrower slabs), there is an interplay between entropy and the Hooke terms in the free energy, and in some cases $f_L < f_{L+1}$. This is for example seen in figure 6 in the data for $L = 3$ and $L = 4$ for the knot type 4_1 . One may also verify that $\mathcal{W}_{4_1} = 36k + T \log(456/185)$.

The results for five crossing knots 5_*^+ and six crossing knots are illustrated in figures 7 and 8.

Our numerical data on seven and eight crossings knots in tables 5 and 6 were used to compute critical forces and \mathcal{W} for each of those knot types. Data on compound knots up to eight crossings are listed in tables 7 and 8, and we similarly determined critical forces and \mathcal{W} for those knot types. The results are shown in tables 1 and 2.

3.2. Discussion

Compressing a lattice knot between two hard walls decreases the entropy of the knot, until the walls are close enough together. Then the lattice knot expands laterally and in length as it finds conformations which can be accommodated in even narrower slabs.

For example, a lattice trefoil loses entropy in \mathbb{S}_L as L is reduced from $L = 4$ to $L = 2$, but then has to increase in length by 2 if it is compressed into \mathbb{S}_1 . This stretching of the lattice knot to a longer length changes its entropic properties, and may even increase its entropy, as the longer lattice polygon may be able to explore more states. However, the Hooke energy involved in stretching the lattice knot increases the free energy, and also increases the critical force necessary to compress the knot into a narrower slab.

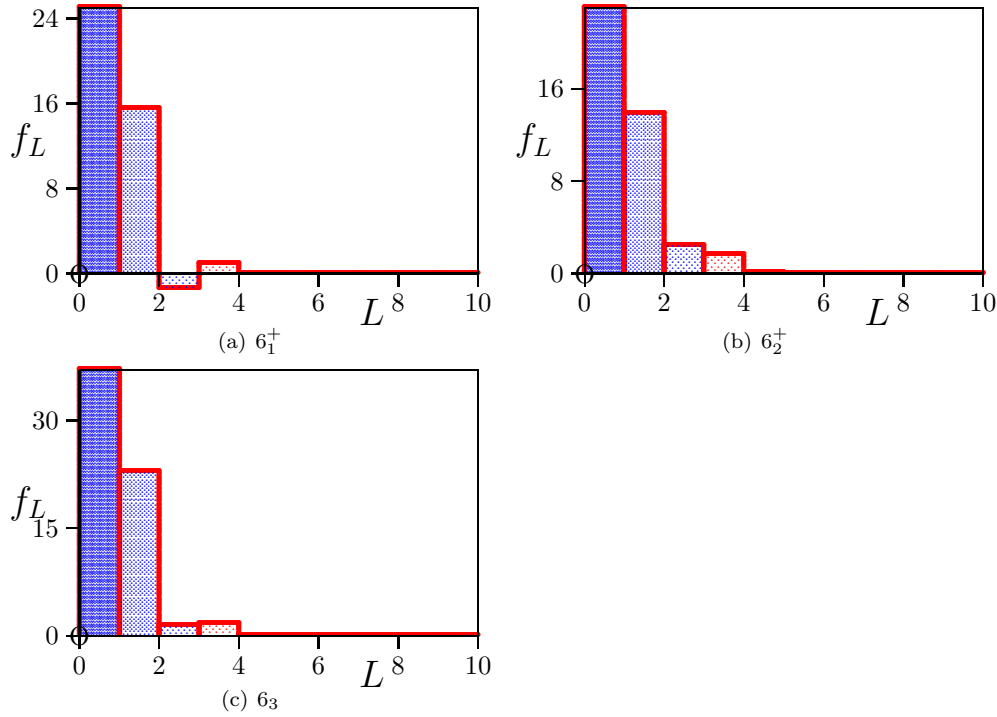


Figure 8. A profile of critical forces f_L for the lattice knots of types 6_1^+ , 6_2^+ and 6_3 . There is no resistance to compression until $L = 5$ in all cases. There are small resistances if $L = 4$. The negative bar between $L = 2$ and $L = 3$ for 6_1^+ shows that a gain in entropy overwhelms the Hooke forces when the lattice knot is compressed from $L = 3$ to $L = 2$ – in fact, no force is necessary, as the entropic force pulls the walls together. Bars in red indicate that the critical forces are due to entropy reduction alone, and blue bars denote a Hooke contribution to the critical force. In this example, $k = 1/4$ and $T = 1$.

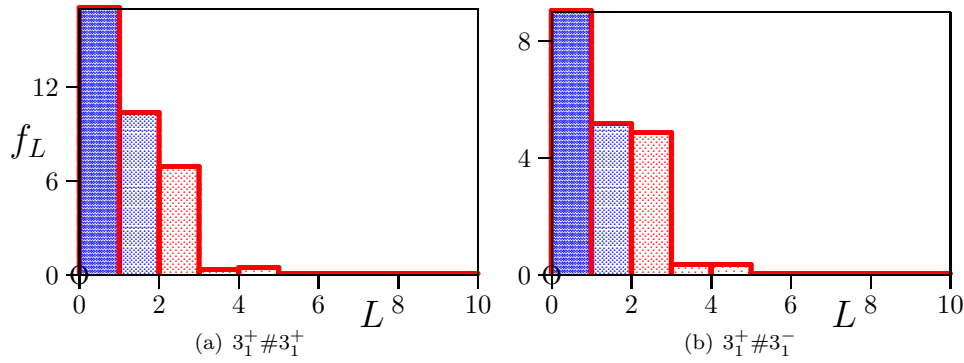


Figure 9. A profile of critical forces f_L for the compound lattice knots of types $3_1^+ \# 3_1^+$ and $3_1^+ \# 3_1^-$. There is no resistance to compression until $L = 5$ in all cases. Bars in red indicate that the critical forces are due to entropy reduction alone, and blue bars denote a Hooke contribution to the critical force. In this example, $k = 1/4$ and $T = 1$.

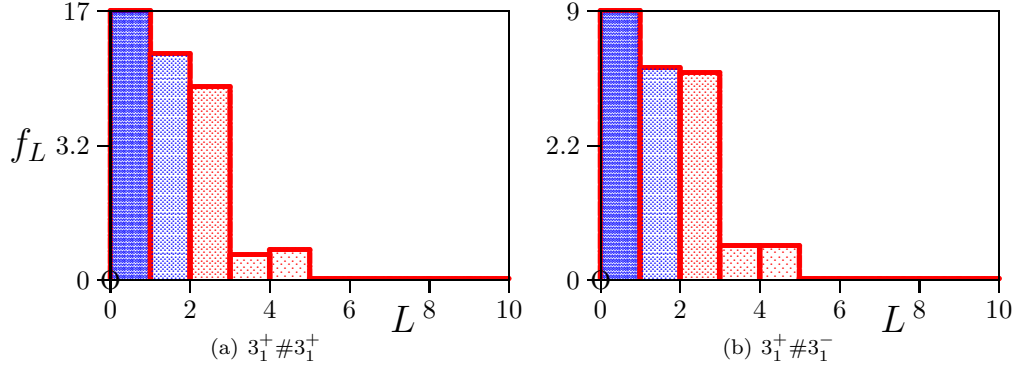


Figure 10. The same data as in figure 9, but with the vertical axes scaled logarithmically to enhance the data at larger values of L .

The critical forces of the trefoil knot 3_1^+ are listed in equation (9). These forces are induced by entropy loss when $L > 2$, but at $L = 2$ a Hooke energy contribution also appears. The sum of these forces gives the total amount of work in an isothermic compression of the lattice knot. We found this to be $\mathcal{W}_{3_1^+} = 4k + T \log(416/9)$. There are two contributions to $\mathcal{W}_{3_1^+}$, namely an entropic and a Hooke contribution. These contributions are equal in magnitude at a critical value of k (or equivalently, a critical value of T). In the case of the trefoil knot this critical value of k is $k_{3_1^+} = [T \log(416/9)]/4 \approx (0.95836 \dots)T$. If $k > k_c$, then the Hooke term dominates $\mathcal{W}_{3_1^+}$ and if $k < k_c$, then the work done has a larger contribution from entropy reduction in the process.

In the case of the figure eight knot, one may similarly determine the critical value of k : $k_{4_1} = (0.02505 \dots)T$. In this case, k_c is very small, and the total amount of work done in compressing the knot to $L = 2$ is dominated by the Hooke term even for relatively small values of k . The two five crossing knots have $k_{5_1^+} = (0.23974 \dots)T$ and $k_{5_2^+} = (0.06167 \dots)T$.

Data on other knots are listed in tables 1 and 2. The critical values of k can be determined by solving for k from the last column in these tables. Observe that some knot types have negative values of k_c , for example, $k_{6_1^+} = -0.015025T$. This implies that a large entropy gain occurs when the knot stretches in length to fit in \mathbb{S}_1 , and this can only be matched by a negative Hooke constant.

	$L = 0$	$L = 1$	$L = 2$	$L = 3$	$L = 4$	$L = 5$	$L = 6$	$L = 7$	\mathcal{W}
0_1	$\log 3$	0	0	0	0	0	0	0	$\log 3$
3_1^+	∞	$4k + \log(\frac{38}{9})$	$\log(\frac{415}{38})$	$\log(\frac{416}{415})$	0	0	0	0	$4k + \log(\frac{416}{9})$
4_1	∞	$32k + \log(\frac{758}{185})$	$4k + \log(\frac{170}{379})$	$\log(\frac{114}{85})$	0	0	0	0	$36k + \log(\frac{456}{185})$
5_1^+	∞	$16k + \log(\frac{95}{9})$	$\log(\frac{34}{19})$	$\log(\frac{206}{85})$	$\log(\frac{417}{415})$	0	0	0	$16k + \log(\frac{139}{3})$
5_2^+	∞	$36k + \log(\frac{3}{26})$	$\log(\frac{1033}{30})$	$\log(\frac{6917}{3099})$	$\log(\frac{7182}{6917})$	0	0	0	$36k + \log(\frac{1197}{130})$
6_1^+	∞	$60k + \log(\frac{3176}{2009})$	$4k + \log(\frac{73}{794})$	$\log(\frac{375}{146})$	$\log(\frac{128}{125})$	0	0	0	$64k + \log(\frac{768}{2009})$
6_2^+	∞	$60k + \log(\frac{15}{46})$	$4k + \log(\frac{373}{90})$	$\log(\frac{1829}{373})$	$\log(\frac{2052}{1829})$	0	0	0	$64k + \log(\frac{171}{23})$
6_3	∞	$84k + \log(\frac{157}{26})$	$16k + \log(\frac{37}{471})$	$\log(\frac{213}{37})$	$\log(\frac{74}{71})$	0	0	0	$100k + \log(\frac{37}{13})$
7_1^+	∞	$36k + \log(\frac{100}{9})$	$\log(\frac{1417}{300})$	$\log(\frac{2890}{1417})$	$\log(\frac{422}{289})$	$\log(\frac{849}{844})$	0	0	$36k + \log(\frac{1415}{9})$
7_2^+	∞	$60k + \log(\frac{62507}{5607})$	$4k + \log(\frac{12924}{62507})$	$\log(\frac{7688}{3231})$	$\log(\frac{41069}{30752})$	$\log(\frac{42045}{41069})$	0	0	$64k + \log(\frac{14015}{1869})$
7_3^+	∞	$84k + \log(\frac{1202}{31})$	$16k + \log(\frac{5}{1803})$	0	$\log(\frac{3}{2})$	0	0	0	$100k + \log(\frac{5}{31})$
7_4^+	∞	$96k + \log(\frac{100}{3361})$	$4k + \log(\frac{1}{20})$	$\log(\frac{16}{5})$	$\log(\frac{21}{16})$	0	0	0	$100k + \log(\frac{21}{3361})$
7_5^+	∞	$96k + \log(\frac{52}{115})$	$4k + \log(\frac{5}{104})$	$\log(\frac{581}{15})$	$\log(\frac{591}{581})$	0	0	0	$100k + \log(\frac{197}{230})$
7_6^+	∞	$96k + \log(\frac{220}{731})$	$4k + \log(\frac{4}{11})$	$\log(\frac{323}{16})$	$\log(\frac{2127}{1615})$	0	0	0	$100k + \log(\frac{2127}{731})$
7_7^+	∞	$108k + \log(2248)$	$32k + \log(\frac{161}{1124})$	$4k + \log(\frac{7}{46})$	$\log(\frac{9}{7})$	0	0	0	$144k + \log(63)$
$3_1^+ \# 3_1^+$	∞	$64k + \log(\frac{4}{1215})$	$\log(975)$	$\log(\frac{2623}{1950})$	$\log(\frac{3826}{2623})$	0	$\log(\frac{1914}{1913})$	0	$64k + \log(\frac{2552}{405})$
$3_1^+ \# 3_1^-$	∞	$16k + \log(\frac{28}{9})$	$\log(\frac{1011}{8})$	$\log(\frac{3274}{2359})$	$\log(\frac{6839}{4911})$	0	$\log(\frac{13679}{13678})$	$\log(\frac{13680}{13679})$	$16k + \log(760)$
$3_1^+ \# 4_1$	∞	$60k + \log(\frac{3434}{1509})$	$4k + \log(\frac{3559}{1717})$	$\log(\frac{16181}{7118})$	$\log(\frac{21026}{16181})$	$\log(\frac{11241}{10513})$	0	0	$64k + \log(\frac{7494}{503})$
$3_1^+ \# 5_1^+$	∞	$64k + \log(\frac{10}{27})$	$\log(395)$	$\log(\frac{53}{25})$	$\log(\frac{4464}{4187})$	$\log(\frac{4183}{2976})$	$\log(\frac{4187}{4183})$	0	$64k + \log(\frac{4187}{9})$
$3_1^+ \# 5_1^-$	∞	$36k + \log(\frac{197}{18})$	$\log(\frac{3374}{197})$	$\log(\frac{12431}{3374})$	$\log(\frac{15328}{12431})$	$\log(\frac{35447}{30656})$	$\log(\frac{35547}{35447})$	0	$36k + \log(\frac{11849}{12})$
$3_1^+ \# 5_2^+$	∞	$64k + \log(\frac{235}{18802})$	$\log(\frac{91191}{235})$	$\log(\frac{273449}{91191})$	$\log(\frac{398758}{273449})$	$\log(\frac{454641}{398758})$	$\log(\frac{453271}{151547})$	0	$64k + \log(\frac{459813}{18802})$
$3_1^+ \# 5_2^-$	∞	$96k - \log(246)$	$4k + \log(\frac{110}{7})$	$\log(\frac{113}{55})$	$\log(\frac{165}{113})$	0	0	0	$100k + \log(\frac{55}{287})$
$4_1 \# 4_1$	∞	$60k + \log(\frac{5477}{100})$	$4k + \log(\frac{5076}{5477})$	$\log(\frac{21601}{5076})$	$\log(\frac{38653}{21601})$	$\log(\frac{41515}{38653})$	$\log(\frac{41853}{41515})$	0	$64k + \log(\frac{41853}{100})$

Table 1. Critical forces f_L for knots up to seven crossings and for compound knot types up to eight crossings. The last column is the maximum amount of useful work which can be extracted if the lattice knot expands against the hard walls of the slab, pushing them apart from $L = 1$. In all these cases we set $T = 1$.

	$L = 0$	$L = 1$	$L = 2$	$L = 3$	$L = 4$	$L = 5$	$L = 6$	$L = 7$	\mathcal{W}
8_1^+	∞	$96k + \log(\frac{254}{2145})$	$4k + \log(\frac{274}{635})$	$\log(\frac{1003}{274})$	$\log(\frac{2787}{2006})$	$\log(\frac{989}{929})$	0	0	$100k + \log(\frac{989}{3575})$
8_2^+	∞	$84k + \log(\frac{73714}{649})$	$16k + \log(\frac{1291}{36857})$	$\log(\frac{3248}{1291})$	$\log(\frac{5263}{3248})$	$\log(\frac{5730}{5263})$	0	0	$100k + \log(\frac{11460}{649})$
8_3	∞	$128k + \log(\frac{500}{2273})$	$16k + \log(\frac{1}{250})$	0	$\log(\frac{3}{2})$	0	0	0	$144k + \log(\frac{3}{2273})$
8_4^+	∞	$96k + \log(\frac{140}{297})$	$4k + \log(\frac{23}{119})$	$\log(\frac{933}{115})$	$\log(\frac{2933}{1866})$	$\log(\frac{2991}{2933})$	0	0	$100k + \log(\frac{1994}{1683})$
8_5^+	∞	$64k + \log(\frac{102047}{18})$	$32k + \log(\frac{1236}{102047})$	$4k + \log(\frac{8}{103})$	$\log(\frac{3}{2})$	0	0	0	$100k + 3 \log(2)$
8_6^+	∞	$140k - \log(1205)$	$\log(3023)$	$4k + \log(\frac{460}{3023})$	$\log(\frac{3}{2})$	0	0	0	$144k + \log(\frac{138}{241})$
8_7^+	∞	$160k + \log(\frac{6172}{2429})$	$36k + \log(\frac{1}{6172})$	$\log(2)$	$\log(\frac{3}{2})$	0	0	0	$196k + \log(\frac{3}{2429})$
8_8^+	∞	$128k + \log(\frac{347}{1696})$	$12k + \log(\frac{5035}{347})$	$4k + \log(\frac{26}{1007})$	$\log(\frac{3}{2})$	0	0	0	$144k + \log(\frac{195}{1696})$
8_9	∞	$128k + \log(\frac{355}{318})$	$16k + \log(\frac{20}{213})$	$\log(\frac{147}{10})$	$\log(\frac{3}{2})$	$\log(\frac{3541}{2940})$	0	0	$144k + \log(\frac{3541}{1272})$
8_{10}^+	∞	$108k + \log(\frac{2982}{13})$	$32k + \log(\frac{221}{1988})$	$4k + \log(\frac{70}{663})$	$\log(\frac{3}{2})$	0	0	0	$144k + \log(\frac{105}{26})$
8_{11}^+	∞	$128k + \log(\frac{453}{183})$	$12k + \log(\frac{5066}{453})$	$4k + \log(\frac{4}{2533})$	$\log(\frac{3}{2})$	0	0	0	$144k + \log(\frac{3}{122})$
8_{12}	∞	$128k + \log(\frac{2897}{183})$	$16k + \log(\frac{18}{14485})$	$\log(6)$	$\log(\frac{3}{2})$	0	0	0	$144k + \log(\frac{54}{305})$
8_{13}^+	∞	$180k + \log(\frac{95}{9987})$	$16k - \log(19)$	$\log(\frac{537}{5})$	$\log(\frac{802}{537})$	$\log(\frac{408}{401})$	0	0	$196k + \log(\frac{272}{3329})$
8_{14}^+	∞	$180k + \log(\frac{172}{1475})$	$12k + \log(\frac{77}{86})$	$4k + \log(\frac{3}{77})$	$\log(\frac{3}{2})$	0	0	0	$196k + \log(\frac{9}{1475})$
8_{15}^+	∞	$84k + \log(55)$	$16k + \log(\frac{282}{55})$	$\log(\frac{3047}{564})$	$\log(\frac{5013}{3047})$	0	0	0	$100k + \log(\frac{5013}{2})$
8_{16}^+	∞	$220k + \log(\frac{73}{2045})$	$32k + \log(\frac{3}{73})$	$4k + \log(2/3)$	$\log(\frac{3}{2})$	0	0	0	$256k + \log(\frac{3}{2045})$
8_{17}	∞	$220k + \log(\frac{518}{3771})$	$32k + \log(\frac{231}{74})$	$4k + \log(\frac{557}{539})$	$\log(\frac{1098}{557})$	$\log(\frac{554}{549})$	0	0	$256k + \log(\frac{1108}{1257})$
8_{18}	∞	$260k + \log(\frac{189}{8})$	$48k + \log(\frac{17000}{189})$	$16k + \log(\frac{37}{2125})$	$\log(3)$	0	0	0	$324k + \log(111)$
8_{19}^+	∞	$32k + \log(\frac{1656}{163})$	$4k + \log(\frac{283}{414})$	$\log(\frac{4677}{283})$	$\log(\frac{583}{559})$	0	0	0	$36k + \log(\frac{6996}{163})$
8_{20}^+	∞	$60k + \log(\frac{318}{29})$	$4k + \log(\frac{5}{159})$	$\log(2)$	$\log(\frac{3}{2})$	0	0	0	$64k + \log(\frac{30}{29})$
8_{21}^+	∞	$60k + \log(30)$	$4k + \log(\frac{857}{180})$	$\log(\frac{6375}{857})$	$\log(\frac{467}{425})$	0	0	0	$64k + \log(\frac{2335}{2})$

Table 2. Critical forces f_L for knots with eight crossings. The last column is the maximum amount of useful work which can be extracted if the lattice knot expands against the hard walls of the slab, pushing them apart from $L = 1$. In all these cases we set $T = 1$.

4. A grafted lattice knot pushed by a force

In this section we consider the model inspired by figure 2: An external force f compresses a grafted lattice knot onto a hard wall. If $p_n(h, K)$ is the number of such lattice knots with highest vertices at height h above the bottom wall and length $n_{h;K}$, then the partition function is given by

$$Z(f) = \sum_{n,h=0}^{\infty} p_{n_{h;K}}(h, K) e^{-E_h - fh} \quad (11)$$

where $n_{h;K} = \min_{L \leq h} \{n_{L,K}\}$ is the minimal length of the polygons in \mathbb{S}_L for all $L \leq h$. For example, $n_{1;3_1^+} = 26$ and $n_{h;3_1^+} = 24$ for all $h > 1$.

In the partition function, positive values of f mean that the vertices in the top layer are pushed towards the bottom wall, and negative values f mean that the force is pulling the vertices in the top layer from the bottom wall. Observe that we put the Boltzman factor $k_B T = 1$ in this definition, and so use lattice units throughout.

The function E_h is an energy of the lattice knot. We shall again use a Hooke energy for the polygons, namely

$$E_h = k(n_{h;K} - n_K)^2. \quad (12)$$

In addition, we assume a low temperature approximation, namely that only polygons of the shortest length in \mathbb{S}_L contribute to $Z(f)$ for all L . That is, in the case of 3_1^+ , only polygons of lengths 24 and 26 (when $h = 1$) contribute. This approximation is also valid in the regime that the Hooke constant k is large.

In other word, the low temperature and large Hooke constant approximation of the partition function is

$$Z^*(f) = \sum_{h=0}^{\infty} p_{n_{h,K}}(h, K) e^{-k(n_{h,K} - n_K)^2 - fh}. \quad (13)$$

For $f < 0$ we observe that the polygon is pulled by its highest vertices from the bottom wall, and that it will stretch in length if the forces overcome the tensile strength of the edges. Stretching the edges in this way will cause the Hooke energy term to increase quadratically in $n \propto h$, while the force f couples only linearly in with h . Thus, this regime will be a purely Hooke regime, provided that k is large enough.

Thus, we obtain a model of fixed length lattice knots, which may stretch to longer states if pushed against the bottom wall by large forces to accommodate itself into a conformation with small h .

The (extensive) free energy in this model is given by

$$\mathcal{F}_f = \log Z^*(f) \quad (14)$$

and its derivatives give the thermodynamic observables of the model. For example, the mean height of the grafted lattice knot is

$$\langle h \rangle_K = -\frac{d\mathcal{F}_f}{df} = \frac{\sum_{h=0}^{\infty} h p_n(K; h) e^{-k(n_{h,K} - n_K)^2 - fh}}{Z^*(f)}, \quad (15)$$

while the second derivative

$$\kappa_K = -\frac{d \log \langle h \rangle_K}{df} = -\frac{1}{\langle h \rangle_K} \frac{d \langle h \rangle_K}{df} \quad (16)$$

is the fractional rate of change in mean height with f , and is a measure of the linear compressibility of the lattice knot due to a force acting on its highest vertices.

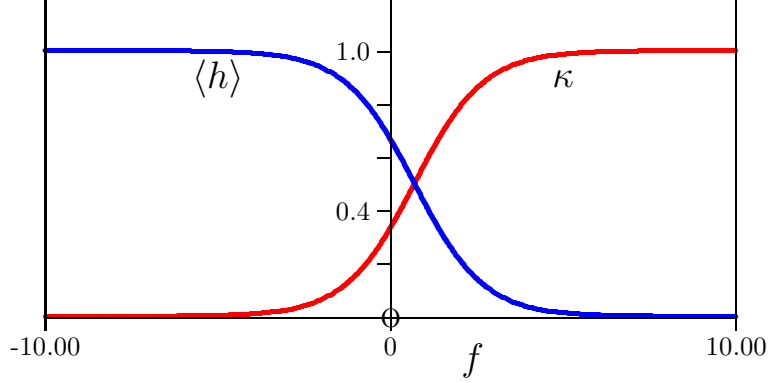


Figure 11. The mean height $\langle h \rangle_{0_1}$ (red curve) and compressibility κ_{0_1} (blue curve) as a function of f for the unknot 0_1 . For negative values of f (pulling forces) the mean height is 1, and as the lattice knot is compressed into pushing forces, its mean height decreases until it approaches zero. Note that $\langle h \rangle = 2/3$ if $f = 0$.

The data in tables 5 and 6 can be used to determine κ_K . For example, for the unknot grafted to the bottom wall, one has $n_{h,K} = n_{L,K} = 4$ if $L = h = 0$ or $L = h = 1$. Thus, we determine the partition function in this case to be

$$Z_{0_1}^*(f) = 1 + 2e^{-f} \quad (17)$$

since $E_h = 0$ for both $h = 0$ and $h = 1$ in this case. Observe that $p_4(0, 0_1) = 1$ and $p_4(1, 0_1) = 2$ in this model.

One may now compute the mean height and κ_{0_1} for the unknot directly from the above. The results are

$$\langle h \rangle_{0_1} = \frac{2e^{-f}}{1 + 2e^{-f}}, \quad \kappa_{0_1} = \frac{1}{1 + 2e^{-f}} \quad (18)$$

and these are plotted in figure 11. If this lattice knot is released from its maximum compressed state in a slab of width $L = 0$, and allowed to expand, then work can be extracted from the expansion. The maximum amount of work which may be extracted is given by the free energy differences between the $L = 0$ slab and the free energy at $f = 0$. This is given by

$$\mathcal{W}_{0_1} = \mathcal{F}_f|_{f=0} - \mathcal{F}_f|_{L=0} = \log 3 - \log 1 = \log 3. \quad (19)$$

This is the same value obtained in the first model.

4.1. Compressing minimal length lattice trefoil knots

By noting that $n_{h,3_1^+} = 24$ if $h \geq 2$ and $n_{1,3_1^+} = 26$ in table 5, one may determine $p_{n(h,3_1^+)}(h, 3_1^+)$ by examining the data in table 6.

In particular, it is apparent that $p_{n(1,3_1^+)}(1, 3_1^+) = 36$ and $p_{n(2,3_1^+)}(2, 3_1^+) = 152$. However, these 152 lattice knots of length $n = 24$ in \mathbb{S}_2 are also counted in \mathbb{S}_3 , and so must be subtracted from the data in column $L = 3$ to obtain $p_{n(3,3_1^+)}(3, 3_1^+)$. In particular, it follows that $p_{n(3,3_1^+)}(3, 3_1^+) = 1660 - 152 = 1508$.

Similarly, one may show that $p_{n(4,3_1^+)}(4, 3_1^+) = 4$ and $p_{n(\geq 5,3_1^+)}(\geq 5, 3_1^+) = 0$. This

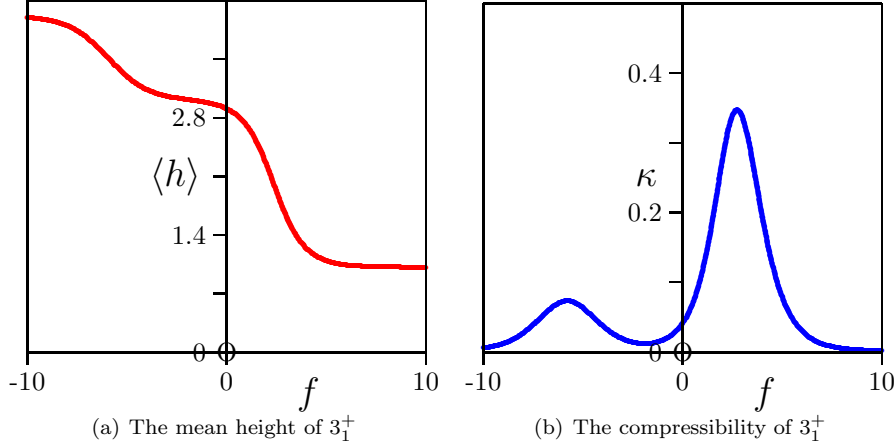


Figure 12. The mean height $\langle h \rangle_{3_1^+}$ and compressibility $\kappa_{3_1^+}$ of grafted lattice knots of type 3_1^+ . Negative forces are pulling forces, stretching the lattice knot from the bottom plane. Positive forces are pushing forces. The mean height decreases in steps from a maximum of about 4 to about 3 at $f = 0$ and then to 1 for large positive f . There are two peaks in $\kappa_{3_1^+}$. The highest peak at positive f corresponds to the pushing force overcoming the Hooke term in \mathcal{F} , increasing the length of the lattice from 24 to 26 and pushing it into a slab of width $L = 1$. In this example, $k = 1/4$.

shows that

$$Z^*(3_1^+) = 36e^{-4k-f} + 152e^{-2f} + 1508e^{-3f} + 4e^{-4f}. \quad (20)$$

The mean height of the lattice knot is

$$\langle h \rangle_{3_1^+} = \frac{9e^{-4k} + 76e^{-f} + 1131e^{-2f} + 4e^{-3f}}{9e^{-4k} + 38e^{-f} + 377e^{-2f} + e^{-3f}} \quad (21)$$

The (linear) compressibility of the lattice knot of type 3_1^+ is a more complicated expression, given by

$$\kappa_{3_1^+} = \frac{(342 + 13572e^{-f} + 81e^{-2f})e^{-4k-f} + (14326 + 152e^{-f} + 377e^{-2f})e^{-3f}}{(9e^{-4k} + 76e^{-f} + 1131e^{-2f} + 4e^{-3f})(9e^{-4k} + 38e^{-f} + 377e^{-2f} + e^{-3f})}.$$

In figures 12 and 13 the mean height and $\kappa_{3_1^+}$ are plotted as a function of the force for $k = 1/4$ (figure 12) and $k = 4/3$ (figure 13). In figure 12 the mean height decreases to $L = 1$ in two steps, the first at negative (pulling) forces, and the second a step from a height of roughly $h = 3$ to $h = 1$. In this step (which shows up as a peak in figure 12(b)) the polygon is squeezed into \mathbb{S}_1 as the force overcomes both the entropy reduction and Hooke term.

Increasing the Hooke constant k produces graphs similar to figure 13. There are now three peaks in κ , each corresponding to a reduction of the lattice knot from height h to height $h - 1$ as the applied force first overcomes entropy and then the Hooke energy to push the lattice knot into \mathbb{S}_1 .

The total amount of work done by letting the lattice polygon expand at zero force from its maximal compressed state in $L = 1$ is given by $\mathcal{W}_{3_1^+} = \mathcal{F}_f|_{L=1} - \mathcal{F}_f|_{f=0}$. This gives

$$\mathcal{W}_{3_1^+} = \log(1664 + 36e^{-4k}) - \log(36e^{-4k}) = \log\left(\frac{416}{9}e^{4k} + 1\right). \quad (22)$$

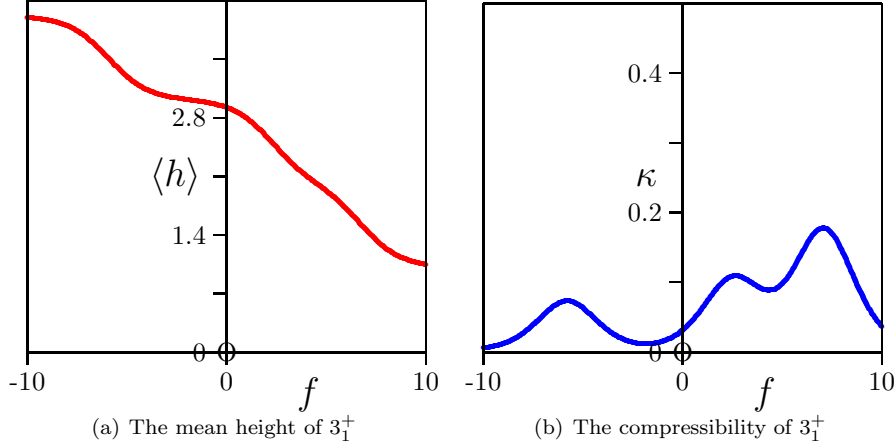


Figure 13. The similar plots to figure 12, but with $k = 4/3$. This larger Hooke energy requires a larger force to push the lattice knots from a $L = 2$ slab into \mathbb{S}_1 . This shows up as a third peak in the κ -graph above.

4.2. Compressing minimal length lattice figure eight knots

The minimal length of a lattice polygon of knot type 4_1 (the figure eight knot) is 36 in \mathbb{S}_1 , 32 in \mathbb{S}_2 and 30 in \mathbb{S}_L with $L \geq 3$. In other words, states with heights 1 or 2 will have a Hooke energy, as they have been stretched in length to squeeze into slabs with small height.

By consulting the data in tables 5 and 6, the partition function of this model can be determined, and it is given by

$$Z^*(4_1) = 1480 e^{-f-36k} + 6064 e^{-2f-4k} + 2720 e^{-3f} + 928 e^{-4f}. \quad (23)$$

The mean height of this lattice knot is given by

$$\langle h \rangle_{4_1} = \frac{185 e^{-36k} + 1516 e^{-f-4k} + 1020 e^{-2f} + 464 e^{-3f}}{185 e^{-36k} + 758 e^{-f-4k} + 340 e^{-2f} + 116 e^{-3f}} \quad (24)$$

and it is plotted in figure 14(a) for $k = 1/4$. Observe that the mean height decreases in steps with increasing f , from height 4 to height 2, before it is squeezed into \mathbb{S}_1 for sufficiently large values of f .

The compressibility is plotted in figure 14(b), and the two peaks correspond to the decreases in $\langle h \rangle_{4_1}$ in steps. At the peaks, the lattice knot has a maximum response to changes in f . The expression for the compressibility is lengthy and will not be reproduced here.

Finally, the total amount of work done by releasing the knot from \mathbb{S}_1 at zero pressure and letting it expand isothermally, is given by

$$\mathcal{W}_{4_1} = \log \left(\frac{456}{185} e^{36k} + \frac{758}{185} e^{32k} + 1 \right) \quad (25)$$

In the case that $k = 0$, $\mathcal{W}_{3_1^+} \approx 3.855 > 2.023 \approx \mathcal{W}_{4_1}$. In other words, more work is done by the trefoil knot. However, if $k = 1/4$ (and a Hooke term is present), then the relation is the opposite: $\mathcal{W}_{3_1^+} \approx 4.841 < 10/379 \approx \mathcal{W}_{4_1}$. Equality is obtained when $k = 0.06588 \dots$

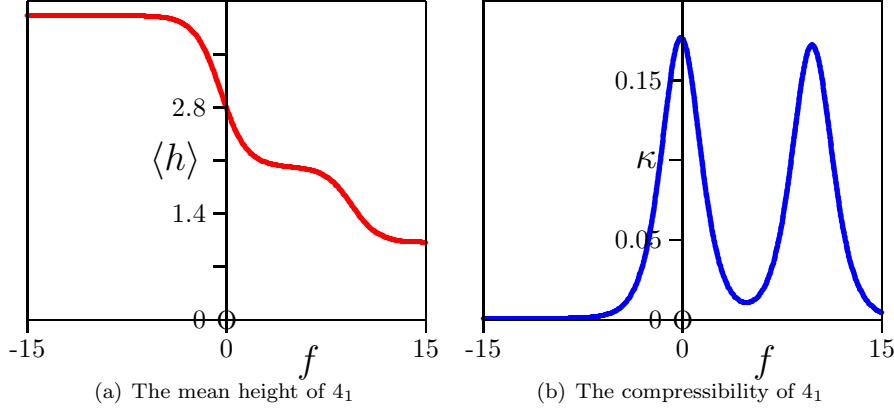


Figure 14. The mean height $\langle h \rangle_{4_1}$ and compressibility κ_{4_1} of grafted lattice knots of type 4_1 . Negative forces are pulling forces, stretching the lattice knot from the bottom plane. Positive forces are pushing forces. The mean height decreases in steps from a maximum of 4 to about 2.8 at $f = 0$ and then to 1 for large positive f . There are two peaks in κ_{4_1} . Both peaks correspond to a reduction in the slab width L as the force first overcomes the Hooke term from $L = 3$ to $L = 2$, and then again at larger pushing forces, the Hooke term from $L = 2$ to $L = 1$. In this example, $k = 1/4$.

4.3. Compressing minimal length lattice knots of types 5_1^+ and 5_2^+

The partition functions of minimal lattice knots of types 5_1^+ and 5_2^+ are given by

$$\begin{aligned} Z^*(5_1^+) &= 72 e^{-f-16k} + 760 e^{-2f} + 600 e^{-3f} + 1936 e^{-4f} + 40 e^{-5f}; \\ Z^*(5_2^+) &= 6240 e^{-f-36k} + 720 e^{-2f} + 24072 e^{-3f} + 30544 e^{-4f} + 2120 e^{-5f}. \end{aligned} \quad (26)$$

These expressions show that the maximum height is 5 while there are Hooke terms for the transition from $h = 2$ to $h = 1$.

The mean heights can be computed, and are given by

$$\begin{aligned} \langle h \rangle_{5_1^+} &= \frac{9 e^{-16k} + 190 e^{-f} + 225 e^{-2f} + 968 e^{-3f} + 25 e^{-4f}}{9 e^{-16k} + 95 e^{-f} + 75 e^{-2f} + 242 e^{-3f} + 5 e^{-4f}}, \\ \langle h \rangle_{5_2^+} &= \frac{780 e^{-36k} + 180 e^{-f} + 9027 e^{-2f} + 15272 e^{-3f} + 1325 e^{-4f}}{780 e^{-36k} + 90 e^{-f} + 3009 e^{-2f} + 3818 e^{-3f} + 265 e^{-4f}}. \end{aligned} \quad (27)$$

\mathcal{W}_K are similar given by

$$\mathcal{W}_{5_1^+} = \log\left(\frac{139}{3} e^{16k} + 1\right) \quad \text{and} \quad \mathcal{W}_{5_2^+} = \log\left(\frac{1197}{130} e^{36k} + 1\right). \quad (28)$$

The results for the 5-crossing knots are plotted in figure 15. The curves for the mean height $\langle h \rangle$ are very similar, with 5_2^+ undergoing a smoother compression with increasing f . The knot type 5_1^+ shows more variation, and this is very visible in the plots for κ in figure 15(b), where there are several sharp peaks for 5_1^+ , but less pronounced changes for 5_2^+ . In both knot types, the Hooke constant is $k = 1/4$.

4.4. Compressing minimal length lattice knots of types 6_1^+ , 6_2^+ and 6_3

The results for 6-crossing knot types are displayed in figure 16. These knot types exhibit more similar behaviour than the two 5-crossing knot types.

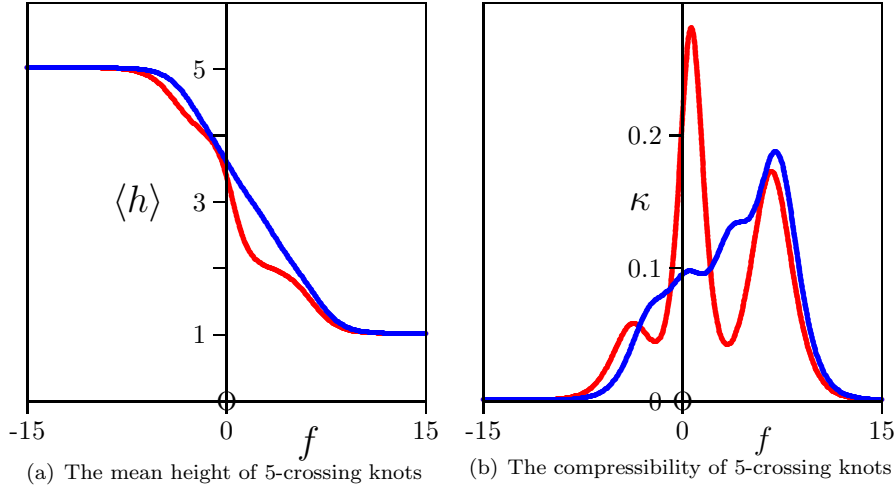


Figure 15. The mean height $\langle h \rangle_{5_*}$ and compressibility κ_{5_*} of grafted lattice knots of types 5_1^+ (red curves) and 5_2^+ (blue curves). The mean height decreases in steps from a maximum of 5 to 1 for large positive f . The transition for 5_2^+ is smoother than for 5_1^+ , which exhibits peaks in κ corresponding to critical forces overcoming the Hooke terms and entropy. There is one low and are two prominent peaks in $\kappa_{5_1^+}$. In this example, $k = 1/4$.

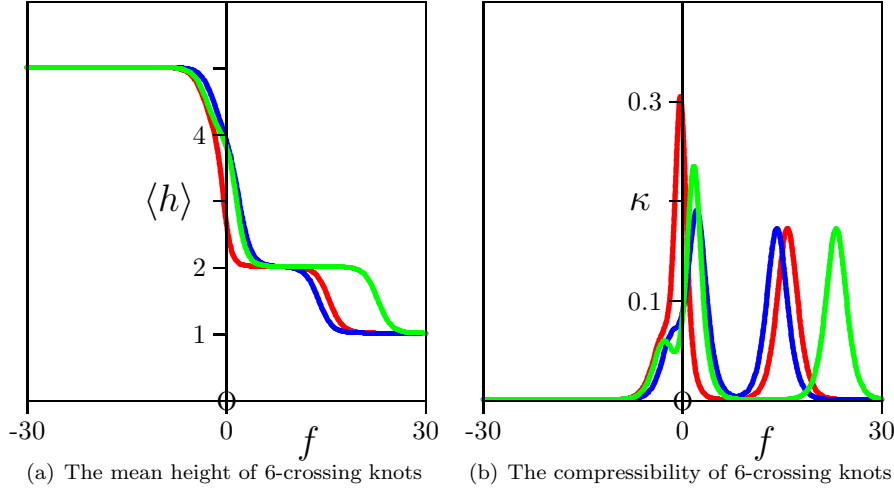


Figure 16. The mean height $\langle h \rangle_{6_*}$ and compressibility κ_{6_*} of grafted lattice knots of types 6_1^+ (red curves), 6_2^+ (blue curves) and 6_3 (green curves). The mean height decreases in steps from a maximum of 5 to 1 for large positive f . These knot types follow a very similar pattern, with 6_3 posing the most resistance to compression. Each knot also exhibits two peaks in κ of similar height. In this example, $k = 1/4$.

Knot	Work
0_1	$\log 3$
3_1^+	$\log \left(\frac{416}{9} e^{4k} + 1 \right)$
4_1	$\log \left(\frac{456}{185} e^{36k} + \frac{758}{185} e^{32k} + 1 \right)$
5_1^+	$\log \left(\frac{139}{3} e^{16k} + 1 \right)$
5_2^+	$\log \left(\frac{1197}{130} e^{36k} + 1 \right)$
6_1^+	$\log \left(\frac{768}{2009} e^{64k} + \frac{3176}{2009} e^{60k} + 1 \right)$
6_2^+	$\log \left(\frac{171}{23} e^{64k} + \frac{15}{46} e^{60k} + 1 \right)$
6_3	$\log \left(\frac{37}{13} e^{100k} + \frac{157}{26} e^{84k} + 1 \right)$
7_1^+	$\log \left(\frac{1415}{9} e^{36k} + 1 \right)$
7_2^+	$\log \left(\frac{14015}{1869} e^{64k} + \frac{62507}{5607} e^{60k} + 1 \right)$
7_3^+	$\log \left(\frac{5}{31} e^{100k} + \frac{1202}{31} e^{84k} + 1 \right)$
7_4^+	$\log \left(\frac{21}{3361} e^{100k} + \frac{100}{3361} e^{96k} + 1 \right)$
7_5^+	$\log \left(\frac{197}{230} e^{100k} + \frac{52}{115} e^{96k} + 1 \right)$
7_6^+	$\log \left(\frac{2127}{731} e^{100k} + \frac{220}{731} e^{96k} + 1 \right)$
7_7^+	$\log \left(63 e^{144k} + 322 e^{140k} + 2248 e^{108k} + 1 \right)$
8_1^+	$\log \left(\frac{989}{3575} e^{100k} + \frac{254}{2145} e^{96k} + 1 \right)$
8_2^+	$\log \left(\frac{11460}{649} e^{100k} + \frac{73714}{649} e^{84k} + 1 \right)$
8_3	$\log \left(\frac{3}{2273} e^{144k} + \frac{500}{2273} e^{128k} + 1 \right)$
8_4^+	$\log \left(\frac{1994}{1683} e^{100k} + \frac{140}{297} e^{96k} + 1 \right)$
8_5^+	$\log \left(8 e^{100k} + \frac{206}{3} e^{96k} + \frac{102047}{18} e^{64k} + 1 \right)$
8_6^+	$\log \left(\frac{138}{241} e^{144k} + \frac{1}{1205} e^{140k} + 1 \right)$
8_7^+	$\log \left(\frac{3}{2429} e^{196k} + \frac{6172}{2429} e^{160k} + 1 \right)$
8_8^+	$\log \left(\frac{195}{1696} e^{144k} + \frac{95}{32} e^{140k} + \frac{347}{1696} e^{128k} + 1 \right)$
8_9^+	$\log \left(\frac{245}{106} e^{144k} + \frac{355}{318} e^{128k} + 1 \right)$
8_{10}^+	$\log \left(\frac{105}{26} e^{144k} + \frac{51}{2} e^{140k} + \frac{2982}{13} e^{108k} + 1 \right)$
8_{11}^+	$\log \left(\frac{3}{122} e^{144k} + \frac{2533}{244} e^{140k} + \frac{453}{488} e^{128k} + 1 \right)$
8_{12}^+	$\log \left(\frac{54}{305} e^{144k} + \frac{2897}{183} e^{128k} + 1 \right)$
8_{13}^+	$\log \left(1632 e^{144k} + 190 e^{128k} + 1 \right)$
8_{14}^+	$\log \left(\frac{9}{1475} e^{196k} + \frac{154}{1475} e^{192k} + \frac{172}{1475} e^{180k} + 1 \right)$
8_{15}^+	$\log \left(\frac{5013}{2} e^{100k} + 55 e^{84k} + 1 \right)$
8_{16}^+	$\log \left(\frac{3}{2045} e^{256k} + \frac{3}{2045} e^{252k} + \frac{73}{2045} e^{220k} + 1 \right)$
8_{17}^+	$\log \left(\frac{1108}{1257} e^{256k} + \frac{539}{1257} e^{252k} + \frac{518}{3771} e^{220k} + 1 \right)$
8_{18}^+	$\log \left(111 e^{324k} + 2125 e^{308k} + \frac{189}{8} e^{260k} + 1 \right)$
8_{19}^+	$\log \left(\frac{6996}{163} e^{36k} + \frac{1656}{163} e^{32k} + 1 \right)$
8_{20}^+	$\log \left(\frac{30}{29} e^{64k} + \frac{318}{29} e^{60k} + 1 \right)$
8_{21}^+	$\log \left(\frac{2335}{2} e^{64k} + 30 e^{60k} + 1 \right)$

Table 3. The work done by releasing the lattice knot in \mathbb{S}_1 and letting it expand to equilibrium at zero pressure.

4.5. Discussion

The compression of lattice knots typically show a few peaks in the compressibility. Since the compressibility is defined as the fractional change in the width of the

Knot	Work
$3_1^+ \# 3_1^+$	$\log \left(\frac{2552}{405} e^{64k} + 1 \right)$
$3_1^+ \# 3_1^-$	$\log \left(760 e^{16k} + 1 \right)$
$3_1^+ \# 4_1$	$\log \left(\frac{7494}{503} e^{64k} + \frac{3434}{1509} e^{60k} + 1 \right)$
$3_1^+ \# 5_1^+$	$\log \left(\frac{4187}{9} e^{64k} + 1 \right)$
$3_1^+ \# 5_1^-$	$\log \left(\frac{11849}{12} e^{36k} + 1 \right)$
$3_1^+ \# 5_2^+$	$\log \left(\frac{459813}{18802} e^{64k} + 1 \right)$
$3_1^+ \# 5_2^-$	$\log \left(\frac{55}{287} e^{100k} + \frac{1}{246} e^{96k} + 1 \right)$
$4_1 \# 4_1$	$\log \left(\frac{41853}{100} e^{64k} + \frac{5477}{100} e^{60k} + 1 \right)$

Table 4. The work done by releasing the lattice knot in \mathbb{S}_1 and letting it expand to equilibrium at zero pressure.

lattice knot with incrementing force, a high compressibility corresponds to a “soft” lattice knot, and a low compressibility to a “hard” lattice knot. The peaks observed in figures from figure 12 to figure 16 correspond to values of f where the lattice knots are soft.

Our general observation is that the compressibility of lattice knots in this model is not monotonic: That is, the lattice knot does not become increasingly more resistant to further compression with increasing force. Instead, it may alternately become more or less resistant to compression, as the compressibility goes through peaks (“soft regimes”) and troughs (“hard regimes”).

The work done by releasing the lattice knot in \mathbb{S}_1 and letting it expand at zero pressure was computed above for knots up to 5-crossings. For example, if the lattice unknot is placed in \mathbb{S}_0 and allowed to expand isothermically to equilibrium at $f = 0$, then $\mathcal{W}_{0_1} = \log 3$.

A similar calculation gave $\mathcal{W}_{3_1^+} = \log \left(\frac{416}{9} e^{4k} + 1 \right)$ for expansion from \mathbb{S}_1 , and expressions were also determined for other knot types. The results are given in tables 3 and 4 for the remaining knot types.

Observe that these expressions are different from those in the model in section 3: There the data were obtained by computing the sum over all the critical forces. In each case the minimal values of the forces required to overcome resistance by the squeezed polygon were determined. This is a different process to the above, where the lattice knots are placed in \mathbb{S}_1 and then allowed to expand isothermically to equilibrium. The total work was obtained by computing the free energy difference between the initial and final states.

Finally, we examined the effect of the Hooke parameter k by comparing \mathcal{W} for two different values of k , namely $k = 1/4$ and $k = 1$. For each knot type, the point $(\mathcal{W}_{k=1/4}, \mathcal{W}_{k=1})$ is plotted as a scatter plot in figure 17. These points line up along a band, indicating that the Hooke term makes a significant contribution to the free energy.

5. Conclusions

In this paper we presented data on minimal length lattice polygons grafted to the bottom walls of slabs \mathbb{S}_L . We collected data on these polygons by implementing the GAS-algorithm for knotted lattice polygons in a slab in the lattice, and sieving out

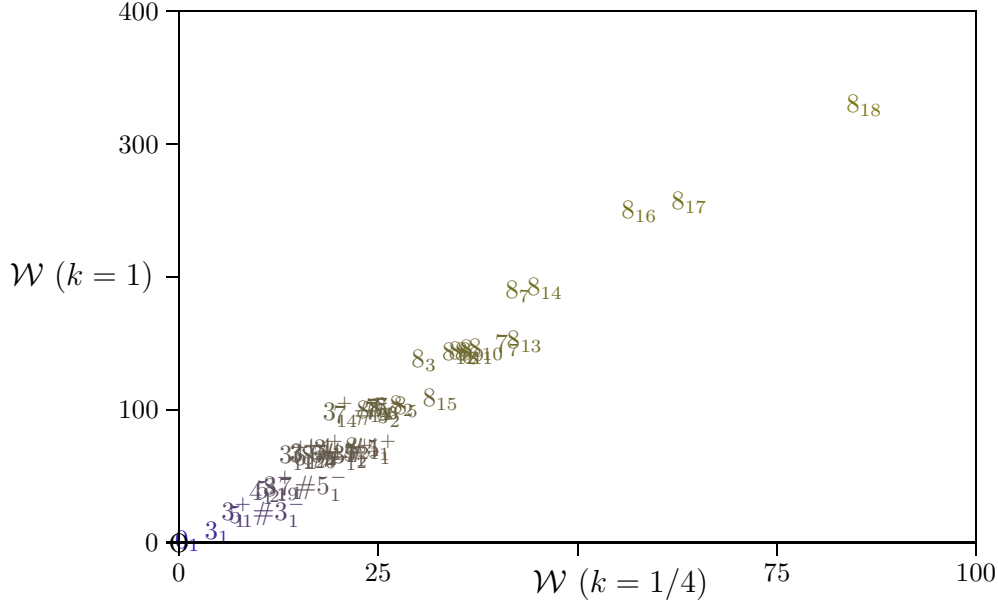


Figure 17. A scatter plot of \mathcal{W} with $k = 1/4$ (horizontal axis) and $k = 1$, (vertical axis). The data for prime knot types accumulate along a band, indicating that the Hooke term makes a significant contribution to the free energy.

minimal length polygons. Our data were presented in tables 5 and 6 for prime knot types, and tables 7 and 8 for compound knot types. Our results verify, up to single exceptions, the data obtained in reference [8].

We determined the compressibility properties of minimal lattice polygons in two ensembles. The first was a model of a ring polymer grafted to the bottom wall of a slab with hard walls, and squeezed by the top wall into a narrower slab.

The second was a model of a ring polymer grafted to a hard wall, and then pushed by a force f towards the bottom wall.

In these models we determined free energies, from which thermodynamic quantities were obtained. In the first model we computed the critical forces which squeeze the lattice polygons into narrower slabs, and we computed the total amount of work that would be done if the lattice polygon was squeezed into \mathbb{S}_1 . These data are displayed in tables 1 and 2.

The profiles of critical forces in this model are dependent on knot types, and generally increases with decreasing values of L . The dependency on knot type shows that entanglements in the lattice knot, in addition to the Hooke term and the entropy, plays a role in determining the resistance of the lattice knot to be squeezed in ever thinner slabs.

We examined the mean height and compressibility profiles for some simple knot types in section 4. The amount of work done by expanding expanding lattice knots from maximal compression at zero force was also determined, and the results were listed in table 3 and 4.

In contrast with the results in section 3, we computed the compressibility of lattice knots as a function of the applied force in section 4. Our results show that the compressibility is dependent on the knot type and the Hooke energy and is not

a monotonic function of the applied force. In many cases there are peaks in the compressibility where the lattice knot becomes (relatively) softer (more compressible) with increasing force. This may feature may be dependent on either the entanglements, or the loss of entropy, or the Hooke term, or on a combination of these. These observations indicate that such peaks may be seen in some conditions when knotted ring polymers are compressed.

Finally, the inclusion of other energy terms, for example a bending term, or a binding term to the walls of the slab, can be done. We expect such additional terms to have an effect on our results. For example, a bending energy will make the lattice knot more rigid and less compressible, increasing the critical forces computed in section 3, and reducing the heights of the peaks seen in the compressibility in section 4. A further generalisation would be to simulate lattice knots in other confined spaces, for example in pores or in channels. Such models pose unique questions, since the algorithm is not known to be irreducible.

Acknowledgements

EJJvR and AR acknowledge support in the form of NSERC Discovery Grants from the Government of Canada.

Bibliography

- [1] C. Aragão de Carvalho, Caracciolo S., and Fröhlich J. Polymers and $g|\phi|^4$ theory in four dimensions. *Nuclear Physics B*, 215(2):209–248, 1983.
- [2] M. Baiesi, E. Orlandini, and A.L. Stella. Ranking knots of random, globular polymer rings. *Physical Review Letters*, 99(5):58301, 2007.
- [3] B. Berg and D. Foerster. Random paths and random surfaces on a digital computer. *Physics Letters B*, 106(4):323–326, 1981.
- [4] Y. Diao. Minimal knotted polygons on the cubic lattice. *Journal of Knot Theory and its Ramifications*, 2(4):413–425, 1993.
- [5] C.O. Dietrich-Buchecker and J.P. Sauvage. A synthetic molecular trefoil knot. *Angewandte Chemie International Edition in English*, 28(2):189–192, 1989.
- [6] A. Dobay, P.E. Sottas, J. Dubochet, and A. Stasiak. Predicting optimal lengths of random knots. *Letters in Mathematical Physics*, 55(3):239–247, 2001.
- [7] A. Gholami, J. Wilhelm, and E. Frey. Entropic forces generated by grafted semiflexible polymers. *Physical Review E*, 74:041803, Oct 2006.
- [8] K. Ishihara, R. Scharein, Y. Diao, J. Arsuaga, M. Vazquez, and K. Shimokawa. Bounds for the minimum step number of knots confined to slabs in the simple cubic lattice. *Journal of Physics A: Mathematical and Theoretical*, 45:065003, 2012.
- [9] E.J. Janse van Rensburg. Squeezing knots. *Journal of Statistical Mechanics: Theory and Experiment*, 2007(03):P03001, 2007.
- [10] E.J. Janse van Rensburg, E. Orlandini, M.C. Tesi, and S.G. Whittington. Knotting in stretched polygons. *Journal of Physics A: Mathematical and Theoretical*, 41:015003, 2008.
- [11] E.J. Janse van Rensburg and A. Rechnitzer. Generalized atmospheric sampling of self-avoiding walks. *Journal of Physics A: Mathematical and Theoretical*, 42:335001, 2009.
- [12] E.J. Janse van Rensburg and A. Rechnitzer. Generalised atmospheric sampling of knotted polygons. *Journal of Knot Theory and its Ramifications*, 2010.
- [13] E.J. Janse van Rensburg and A. Rechnitzer. The compressibility of minimal lattice knots. *Journal of Statistical Mechanics: Theory and Experiment*, 2012(05):P05003, 2012.

- [14] E.J. Janse van Rensburg and S.G. Whittington. The knot probability in lattice polygons. *Journal of Physics A: Mathematical and General*, 23:3573, 1990.
- [15] E.J. Janse van Rensburg and S.G. Whittington. The bfacf algorithm and knotted polygons. *Journal of Physics A: Mathematical and General*, 24(23):5553, 1991.
- [16] N. Kresge, R.D. Simoni, and R.L. Hill. Unwinding the dna topoisomerase story: the work of james c. wang. *Journal of Biological Chemistry*, 282(22):e17, 2007.
- [17] Z. Liu, J.K. Mann, E.L. Zechiedrich, and H.S. Chan. Topological information embodied in local juxtaposition geometry provides a statistical mechanical basis for unknotting by type-2 dna topoisomerases. *Journal of Molecular Biology*, 361(2):268–285, 2006.
- [18] R. Matthews, A.A. Louis, and J.M. Yeomans. Confinement of knotted polymers in a slit. *Molecular Physics*, 109(7-10):1289–1295, 2011.
- [19] R. Metzler, A. Hanke, P.G. Dommersnes, Y. Kantor, and M. Kardar. Equilibrium shapes of flat knots. *Physical Review Letters*, 88(18):188101, 2002.
- [20] J.P.J. Michels and F.W. Wiegel. On the topology of a polymer ring. *Proceedings of the Royal Society of London. A. Mathematical and Physical Sciences*, 403(1825):269–284, 1986.
- [21] E. Orlandini, A.L. Stella, and C. Vanderzande. Loose, flat knots in collapsed polymers. *Journal of Statistical Physics*, 115(1):681–700, 2004.
- [22] R. Scharein, K. Ishihara, J. Arsuaga, Y. Diao, K. Shimokawa, and M. Vazquez. Bounds for the minimum step number of knots in the simple cubic lattice. *Journal of Physics A: Mathematical and Theoretical*, 42:475006, 2009.
- [23] S.Y. Shaw and J.C. Wang. Knotting of a dna chain during ring closure. *Science*, 260(5107):533–536, 1993.
- [24] M.K. Shimamura and T. Deguchi. Knot complexity and the probability of random knotting. *Physical Review E*, 66:040801, Oct 2002.
- [25] S. Swetman, C. Brett, and M.P. Allen. Phase diagrams of knotted and unknotted ring polymers. *Physical Review E*, 2012.
- [26] W.R. Taylor. A deeply knotted protein structure and how it might fold. *Nature*, 406(6798):916–919, 2000.
- [27] M.C. Tesi, E.J. Janse van Rensburg, E. Orlandini, and S.G. Whittington. Knot probability for lattice polygons in confined geometries. *Journal of Physics A: Mathematical and General*, 27:347, 1994.
- [28] P. Virnau, Y. Kantor, and M. Kardar. Knots in globule and coil phases of a model polyethylene. *Journal of the American Chemical Society*, 127(43):15102–15106, 2005.
- [29] E.L. Zechiedrich, A.B. Khodursky, and N.R. Cozzarelli. Topoisomerase iv, not gyrase, decatenates products of site-specific recombination in *escherichia coli*. *Genes & development*, 11(19):2580–2592, 1997.

Appendix: Numerical Results

Our raw data on the estimates of the exact minimal lengths and number of minimal length lattice knots in \mathbb{S}_L are displayed in tables ??, 7, 6 and 8.

Data on the symmetry classes of lattice knots confined to slabs \mathbb{S}_L . Data are presented in the format $A^a B^b C^c \dots$ denoting a symmetry classes of polygons, each with A members, b symmetry classes of polygons, each with B members, and so on.

Knot	$n_{L,K}$							
	$L = 1$	$L = 2$	$L = 3$	$L = 4$	$L = 5$	$L = 6$	$L = 7$	$L = 8$
0_1	4	4	4	4	4	4	4	4
3_1^+	<u>26</u>	24	24	24	24	24	24	24
4_1	<u>36</u>	<u>32</u>	30	30	30	30	30	30
5_1^+	<u>38</u>	34	34	34	34	34	34	34
5_2^+	<u>42</u>	36	36	36	36	36	36	36
6_1^+	<u>48</u>	<u>42</u>	40	40	40	40	40	40
6_2^+	<u>48</u>	<u>42</u>	40	40	40	40	40	40
6_3	<u>50</u>	<u>44</u>	40	40	40	40	40	40
7_1^+	<u>50</u>	<u>44</u>	44	44	44	44	44	44
7_2^+	<u>54</u>	<u>48</u>	46	46	46	46	46	46
7_3^+	<u>54</u>	<u>48</u>	44	44	44	44	44	44
7_4^+	<u>54</u>	<u>46</u>	44	44	44	44	44	44
7_5^+	<u>56</u>	<u>48</u>	46	46	46	46	46	46
7_6^+	<u>56</u>	<u>48</u>	46	46	46	46	46	46
7_7^+	<u>56</u>	<u>50</u>	<u>46</u>	44	44	44	44	44
8_1^+	<u>60</u>	<u>52</u>	50	50	50	50	50	50
8_2^+	<u>60</u>	<u>54</u>	50	50	50	50	50	50
8_3	<u>60</u>	<u>52</u>	48	48	48	48	48	48
8_4^+	<u>60</u>	<u>52</u>	50	50	50	50	50	50
8_5^+	<u>60</u>	<u>56</u>	<u>52</u>	50	50	50	50	50
8_6^+	<u>62</u>	<u>52</u>	<u>52</u>	50	50	50	50	50
8_7^+	<u>62</u>	<u>54</u>	48	48	48	48	48	48
8_8^+	<u>62</u>	<u>54</u>	<u>52</u>	50	50	50	50	50
8_9	<u>62</u>	<u>54</u>	50	50	50	50	50	50
8_{10}^+	<u>62</u>	<u>56</u>	<u>52</u>	50	50	50	50	50
8_{11}^+	<u>62</u>	<u>54</u>	<u>52</u>	50	50	50	50	50
8_{12}	<u>64</u>	<u>56</u>	52	52	52	52	52	52
8_{13}^+	<u>64</u>	<u>54</u>	50	50	50	50	50	50
8_{14}^+	<u>64</u>	<u>54</u>	<u>52</u>	50	50	50	50	50
8_{15}^+	<u>62</u>	<u>56</u>	52	52	52	52	52	52
8_{16}^+	<u>66</u>	<u>56</u>	<u>52</u>	50	50	50	50	50
8_{17}	<u>68</u>	<u>58</u>	<u>54</u>	52	52	52	52	52
8_{18}	<u>70</u>	<u>60</u>	<u>56</u>	52	52	52	52	52
8_{19}^+	<u>48</u>	<u>44</u>	42	42	42	42	42	42
8_{20}^+	<u>52</u>	<u>46</u>	44	44	44	44	44	44
8_{21}^+	<u>54</u>	<u>48</u>	46	46	46	46	46	46

Table 5. The minimal length of lattice knots of prime knot type to eight crossings confined to slabs of width L . Cases with an increase in minimal length are underlined.

Knot	$p_{n_{L,K}}(K)$							
	$L = 1$	$L = 2$	$L = 3$	$L = 4$	$L = 5$	$L = 6$	$L = 7$	$L = 8$
0_1	3	3	3	3	3	3	3	3
3_1^+	36	152	1660	1664	1664	1664	1664	1664
4_1	1480	6064	2720	3648	3648	3648	3648	3648
5_1^+	72	760	1360	3296	3336	3336	3336	3336
5_2^+	6240	720	24792	55336	57456	57456	57456	57456
6_1^+	8036	12704	1168	3000	3072	3072	3072	3072
6_2^+	2208	720	2984	14632	16416	16416	16416	16416
6_3	1248	7536	592	3408	3552	3552	3552	3552
7_1^+	108	1200	5668	11560	16880	16980	16980	16980
7_2^+	22428	250028	51696	123008	164276	168180	168180	168180
7_3^+	1488	57696	160	160	240	240	240	240
7_4^+	13444	400	20	64	84	84	84	84
7_5^+	5520	2496	120	4648	4728	4728	4728	4728
7_6^+	5848	1760	640	12920	17016	17016	17016	17016
7_7^+	4	8992	1288	196	252	252	252	252
8_1^+	42900	5080	2192	8024	11148	11868	11868	11868
8_2^+	2596	294856	10328	25984	42104	45840	45840	45840
8_3	9092	2000	8	8	12	12	12	12
8_4^+	20196	9520	1840	14928	23464	23928	23928	23928
8_5^+	72	408180	4944	384	384	384	384	384
8_6^+	9640	8	24184	3680	5520	5520	5520	5520
8_7^+	19432	49376	8	16	24	24	24	24
8_8^+	13568	2776	40280	1040	1560	1560	1560	1560
8_9	15264	17040	4920	30584	42492	42492	42492	42492
8_{10}^+	208	47712	5304	560	840	840	840	840
8_{11}^+	3904	3624	40528	64	96	96	96	96
8_{12}	14640	231760	288	1728	2592	2592	2592	2592
8_{13}^+	159792	1520	80	8592	12832	13056	13056	13056
8_{14}^+	59000	6880	6160	240	360	360	360	360
8_{15}^+	16	880	4512	24376	40104	40104	40104	40104
8_{16}^+	32720	1168	48	32	48	48	48	48
8_{17}	60336	8288	25872	26736	52704	53184	53184	53184
8_{18}	32	756	68000	1184	3552	3552	3552	3552
8_{19}^+	163	1656	1132	6708	6996	6996	6996	6996
8_{20}^+	116	1272	40	80	120	120	120	120
8_{21}^+	24	720	3428	25500	28020	28020	28020	28020

Table 6. The number of lattice knots of prime knot type to eight crossings confined to slabs of width L .

Knot	$n_{L,K}$							
	$L = 1$	$L = 2$	$L = 3$	$L = 4$	$L = 5$	$L = 6$	$L = 7$	$L = 8$
$3_1^+3_1^+$	<u>48</u>	40	40	40	40	40	40	40
$3_1^+3_1^-$	<u>44</u>	40	40	40	40	40	40	40
$3_1^+4_1$	<u>54</u>	<u>48</u>	46	46	46	46	46	46
$3_1^+5_1^+$	<u>58</u>	50	50	50	50	50	50	50
$3_1^+5_1^-$	<u>56</u>	50	50	50	50	50	50	50
$3_1^+5_2^+$	<u>60</u>	52	52	52	52	52	52	52
$3_1^+5_2^-$	<u>60</u>	<u>52</u>	50	50	50	50	50	50
4_14_1	<u>60</u>	<u>54</u>	52	52	52	52	52	52

Table 7. The minimal length of lattice knots of compound knot type to eight crossings confined to slabs of width L . Cases with an increase in minimal length are underlined.

Knot	$p_{n_{L,K}}(K)$							
	$L = 1$	$L = 2$	$L = 3$	$L = 4$	$L = 5$	$L = 6$	$L = 7$	$L = 8$
$3_1^+3_1^+$	2430	8	7800	10492	15304	15304	15312	15312
$3_1^+3_1^-$	144	448	56616	78576	109424	109424	109432	109440
$3_1^+4_1$	12072	27472	56944	129448	168208	179856	179856	179856
$3_1^+5_1^+$	216	80	31600	66992	71424	100392	100488	100488
$3_1^+5_1^-$	288	3152	53984	198896	245248	283576	284376	284376
$3_1^+5_2^+$	150416	1880	729528	2187592	3190064	3637128	3678504	3678504
$3_1^+5_2^-$	13776	56	880	1808	2640	2640	2640	2640
4_14_1	800	43816	40608	172808	309224	332120	334824	334824

Table 8. The number of lattice knots of compound knot type to eight crossings confined to slabs of width L .

Knot	Symmetry Classes							
	$L = 1$	$L = 2$	$L = 3$	$L = 4$	$L = 5$	$L = 6$	$L = 7$	$L = 8$
0_1	3^1	3^1	3^1	3^1	3^1	3^1	3^1	3^1
3_1^+	$4^3 8^3$	8^{19}	$4^1 8^3 12^6 24^{65}$	$4^1 8^2 12^7 24^{65}$	$4^1 8^2 12^7 24^{65}$	$4^1 8^2 12^7 24^{65}$	$4^1 8^2 12^7 24^{65}$	$4^1 8^2 12^7 24^{65}$
4_1	$4^{22} 8^{174}$	$8^{750} 16^4$	$16^{116} 24^{36}$	24^{152}	24^{152}	24^{152}	24^{152}	24^{152}
5_1^+	$4^6 8^6$	8^{95}	$4^6 8^{105} 16^{31}$	$12^6 16^5 24^{131}$	$12^6 24^{136}$	$12^6 24^{136}$	$12^6 24^{136}$	$12^6 24^{136}$
5_2^+	$4^{30} 8^{765}$	8^{90}	$4^4 8^{1687} 16^{705}$	$12^4 16^{265} 24^{2127}$	$12^4 24^{2392}$	$12^4 24^{2392}$	$12^4 24^{2392}$	$12^4 24^{2392}$
6_1^+	$4^{43} 8^{983}$	8^{1588}	$8^{112} 16^{17}$	$12^2 16^9 24^{118}$	$12^2 24^{127}$	$12^2 24^{127}$	$12^2 24^{127}$	$12^2 24^{127}$
6_2^+	$4^{18} 8^{267}$	8^{90}	$8^{365} 16^4$	$16^{223} 24^{461}$	24^{684}	24^{684}	24^{684}	24^{684}
6_3	8^{156}	8^{942}	$8^{38} 16^{18}$	$16^{18} 24^{130}$	24^{148}	24^{148}	24^{148}	24^{148}
7_1^+	$4^9 8^9$	8^{150}	$4^1 8^{666} 16^{21}$	$8^7 12^2 16^{674} 24^{29}$	$8^5 12^4 16^{10} 24^{693}$	$12^9 24^{703}$	$12^9 24^{703}$	$12^9 24^{703}$
7_2^+	$4^{41} 8^{2783}$	$4^9 8^{31249}$	$8^{4600} 16^{931}$	$8^{127} 16^{5403} 24^{1481}$	$12^7 16^{488} 24^{6516}$	$12^7 24^{7004}$	$12^7 24^{7004}$	$12^7 24^{7004}$
7_3^+	8^{186}	8^{7212}	16^{10}	16^{10}	24^{10}	24^{10}	24^{10}	24^{10}
7_4^+	$2^6 4^{86} 8^{1636}$	$4^{10} 8^{45}$	$4^1 8^2$	$8^1 16^2 24^1$	$12^1 24^3$	$12^1 24^3$	$12^1 24^3$	$12^1 24^3$
7_5^+	8^{690}	8^{312}	$8^{13} 16^1$	$16^{10} 24^{187}$	24^{197}	24^{197}	24^{197}	24^{197}
7_6^+	8^{731}	8^{220}	8^{80}	$16^{512} 24^{197}$	24^{709}	24^{709}	24^{709}	24^{709}
7_7^+	4^1	$4^{32} 8^{1108}$	$4^{10} 8^{156}$	$12^1 16^7 24^3$	$12^1 24^{10}$	$12^1 24^{10}$	$12^1 24^{10}$	$12^1 24^{10}$
$3_1^+ 3_1^+$	$2^3 4^{36} 8^{285}$	4^2	$8^{303} 16^{336}$	$8^2 12^1 16^{600} 24^{36}$	$12^2 16^1 24^{636}$	$12^2 16^1 24^{636}$	$12^2 24^{637}$	$12^2 24^{637}$
$3_1^+ 3_1^-$	8^{18}	8^{56}	$8^{2050} 16^{2500} 24^9$	$8^1 16^{3856} 24^{703}$	$8^1 24^{4559}$	$8^1 24^{4559}$	$16^1 24^{4559}$	24^{4560}
$3_1^+ 4_1$	8^{1509}	8^{3434}	$8^{4758} 16^{1180}$	$8^{282} 16^{5737} 24^{1475}$	$16^{1456} 24^{6038}$	24^{7494}	24^{7494}	24^{7494}
$3_1^+ 5_1^+$	8^{27}	8^{10}	$8^{3756} 16^{97}$	$8^{36} 16^{4115} 24^{36}$	$16^{3633} 24^{554}$	$16^{12} 24^{4175}$	24^{4187}	24^{4187}
$3_1^+ 5_1^-$	8^{36}	8^{394}	$8^{6006} 16^{371}$	$8^{470} 16^{9745} 24^{1634}$	$16^{4891} 24^{6958}$	$16^{100} 24^{11749}$	24^{11849}	24^{11849}
$3_1^+ 5_2^+$	8^{18802}	8^{235}	$8^{74813} 16^{8189}$	$8^{37388} 16^{11588} 24^{4295}$	$16^{61055} 24^{92216}$	$16^{5172} 24^{148099}$	24^{153271}	24^{153271}
$3_1^+ 5_2^-$	8^{1722}	8^7	8^{110}	$16^{104} 24^6$	24^{110}	24^{110}	24^{110}	24^{110}
$4_1 4_1$	8^{100}	$4^{118} 8^{5418}$	$8^{4466} 16^{305}$	$8^{6873} 16^{6551} 24^{542}$	$12^{30} 16^{3200} 24^{10736}$	$12^{30} 16^{338} 24^{13598}$	$12^{30} 24^{13936}$	$12^{30} 24^{13936}$

Table 9. The symmetry classes of prime lattice knots upto seven crossings, and compound lattice knots upto eight crossings, confined to \mathbb{S}_L with $L \leq 8$.

Knot	Symmetry Classes							
	$L = 1$	$L = 2$	$L = 3$	$L = 4$	$L = 5$	$L = 6$	$L = 7$	$L = 8$
8_1^+	$4^{55}8^{5335}$	8^{635}	8^{274}	$8^1 16^{480} 24^{14}$	$12^1 16^{90} 24^{404}$	$12^1 24^{494}$	$12^1 24^{494}$	$12^1 24^{494}$
8_2^+	$4^{23}8^{313}$	8^{36857}	$8^{1271} 16^{10}$	$8^{594} 16^{1294} 24^{22}$	$16^{467} 24^{1443}$	24^{1910}	24^{1910}	24^{1910}
8_3	$4^3 8^{1135}$	8^{250}	8^1	8^1	12^1	12^1	12^1	12^1
8_4^+	$4^{63}8^{2493}$	8^{1190}	8^{230}	$8^{147} 16^{831} 24^{19}$	$16^{58} 24^{939}$	24^{997}	24^{997}	24^{997}
8_5^+	$2^2 4^5 8^6$	$4^{57} 8^{50994}$	$4^{10} 8^{613}$	16^{24}	16^{24}	16^{24}	16^{24}	16^{24}
8_6^+	8^{1205}	8^1	$8^{3013} 16^5$	16^{230}	24^{230}	24^{230}	24^{230}	24^{230}
8_7^+	8^{2429}	8^{6172}	8^1	16^1	24^1	24^1	24^1	24^1
8_8^+	8^{1696}	8^{347}	$8^{4959} 16^{38}$	16^{65}	24^{65}	24^{65}	24^{65}	24^{65}
8_9	8^{1908}	8^{2130}	$8^{239} 16^{134} 24^{36}$	$8^1 16^{1488} 24^{282}$	$12^1 24^{1770}$	$12^1 24^{1770}$	$12^1 24^{1770}$	$12^1 24^{1770}$
8_{10}^+	8^{26}	8^{5964}	8^{663}	16^{35}	24^{35}	24^{35}	24^{35}	24^{35}
8_{11}^+	8^{488}	8^{453}	$8^{5056} 16^5$	16^4	24^4	24^4	24^4	24^4
8_{12}	8^{1830}	8^{28970}	8^{36}	16^{108}	24^{108}	24^{108}	24^{108}	24^{108}
8_{13}^+	8^{19974}	8^{190}	8^{10}	$8^{121} 16^{316} 24^{107}$	$16^{28} 24^{516}$	24^{544}	24^{544}	24^{544}
8_{14}^+	8^{7375}	8^{860}	$8^{748} 16^{11}$	16^{15}	24^{15}	24^{15}	24^{15}	24^{15}
8_{15}^+	$4^2 8^1$	8^{110}	$4^{10} 8^{559}$	$4^7 8^{350} 12^3 16^{1259} 24^{57}$	$12^{10} 24^{1666}$	$12^{10} 24^{1666}$	$12^{10} 24^{1666}$	$12^{10} 24^{1666}$
8_{16}^+	$4^{14} 8^{4083}$	8^{146}	8^6	16^2	24^2	24^2	24^2	24^2
8_{17}	8^{7542}	8^{1036}	8^{3234}	$8^{1154} 16^{998} 24^{64}$	$16^{60} 24^{2156}$	24^{2216}	24^{2216}	24^{2216}
8_{18}	$4^4 8^2$	$2^6 4^6 8^{90}$	8^{8500}	8^{148}	24^{148}	24^{148}	24^{148}	24^{148}
8_{19}^+	$1^1 2^3 4^9 8^{15}$	8^{207}	$4^{13} 8^{75} 16^{30}$	$8^{12} 12^{13} 16^{30} 24^{249}$	$12^{25} 24^{279}$	$12^{25} 24^{279}$	$12^{25} 24^{279}$	$12^{25} 24^{279}$
8_{20}^+	$4^3 8^{13}$	8^{159}	8^5	16^5	24^5	24^5	24^5	24^5
8_{21}^+	$4^2 8^2$	8^{90}	$4^1 8^{428}$	$12^1 16^{315} 24^{852}$	$12^1 24^{1167}$	$12^1 24^{1167}$	$12^1 24^{1167}$	$12^1 24^{1167}$

Table 10. The symmetry classes of prime lattice knots up to eight crossings, confined to \mathbb{S}_L with $L \leq 8$.